

Exclusive diffractive production of soft photons in pp collisions at the LHC

Piotr Lebiedowicz¹

in collaboration with Otto Nachtmann² and Antoni Szczurek¹

¹ IFJ PAN, Kraków, Poland

² Heidelberg University, Germany



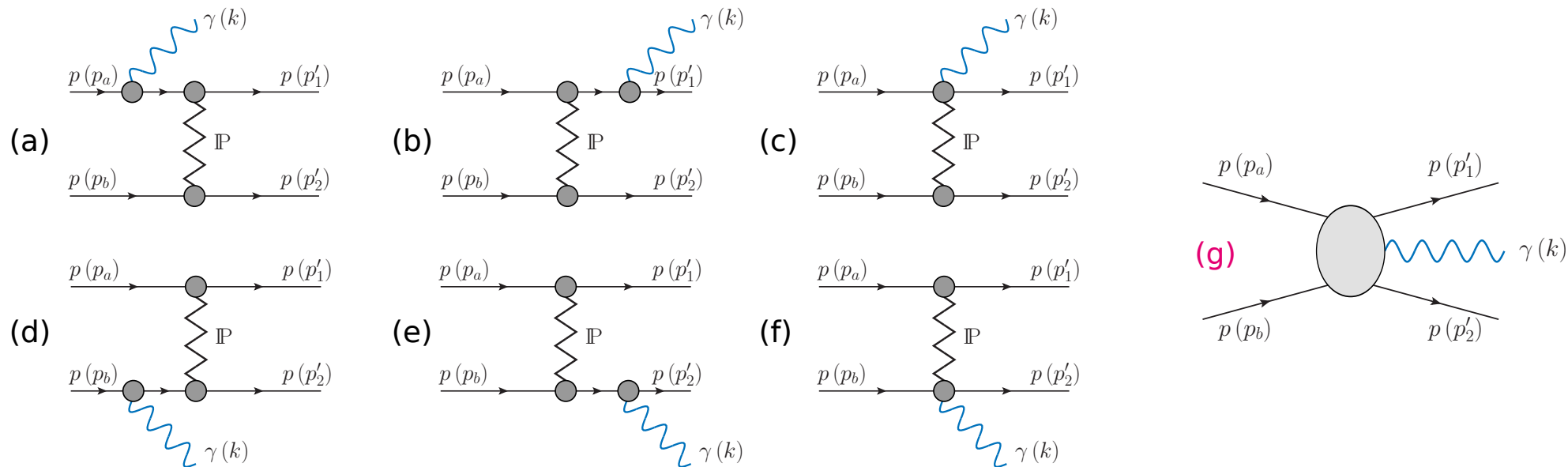
THE HENRYK NIEWODNICZAŃSKI
INSTITUTE OF NUCLEAR PHYSICS
POLISH ACADEMY OF SCIENCES

EMMI Workshop: Soft photons – the higher orders,
26 May 2025, Heidelberg University, Germany

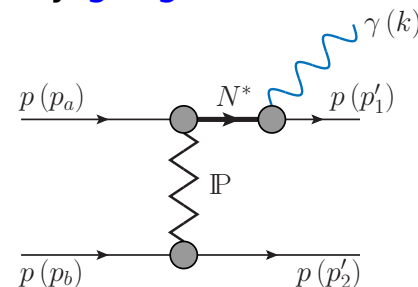
Introduction

- **Inclusive differential production cross-section of forward photons in pp collisions was measured** using RHICf detector and LHCf detector. In the **ATLAS-LHCf combined analysis (ATLAS-CONF-2017-075)** the forward-photon spectra were measured by the LHCf detector and the inner tracking system of the ATLAS detector, which is used to identify diffractive events. In this method, the energy spectrum of photons was obtained in two regions of photon rapidity ($8.81 < y < 8.99$, $y > 10.94$) for events with no charged particles having $p_t > 100$ MeV in $|\eta| < 2.5$.
- **The reaction $pp \rightarrow ppy$ has not been measured yet at the LHC.** Feasibility studies of exclusive diffractive bremsstrahlung cross sections were performed for RHIC energies (Chwastowski et al., Acta Phys. Pol. B46 (2015) 1979) and for LHC energies using the ATLAS forward detectors (Chwastowski et al., EPJC 76 (2016) 354; EPJC 77 (2017) 216).
- A measurement of the soft-photon production at the LHC could shed light on **anomalous soft photons** -- a long-standing discrepancy between the theoretical predictions of the bremsstrahlung (based on the soft-photon theorem) and the measured soft-photon spectra in several hadronic reactions; see Bailhache et al., "Anomalous soft photons: Status and perspectives", Phys. Rept. 1097 (2024) 1.
- Planned upgrade of the ALICE experiment at the LHC (**ALICE 3**, arXiv:2211.02491 [physics.ins-det])
- Exclusive photon-bremsstrahlung processes discussed by our group (Lebiedowicz, Nachtmann, Szczurek):
 $\pi\pi \rightarrow \pi\pi\gamma$ PRD 105 (2022) 014022; Erratum PRD 109 (2024) 099901
 $pp \rightarrow ppy$ PRD 106 (2022) 034023, PRD 107 (2023) 074014, PLB 843 (2023) 138053 ←this talk
 $\pi p \rightarrow \pi p\gamma$ PRD 109 (2024) 094042, PRD 110 (2024) 094028

Formalism



- **Diffractive photon-bremsstrahlung** amplitude contains 6 diagrams. The amplitudes (a, b, d, e) corresponding to photon emission from the external protons are determined by the **off-shell pp elastic scattering amplitude**. The contact terms, (c) and (f), are needed in order to satisfy **gauge-invariance constraints**.
- All **“anomalous” terms** are subsumed in (g).
Will not lead to a singular contribution as $k \rightarrow 0$
(e.g. diffractive excitations of the proton, CEP of photon - fusion processes)



Formalism

The inclusive cross section for the real-photon ($k^2 = 0$) emission

$$d\sigma(pp \rightarrow pp\gamma) = \frac{1}{2\sqrt{s(s-4m_p^2)}} \frac{d^3k}{(2\pi)^3 2k^0} \int \frac{d^3p'_1}{(2\pi)^3 2p'_1{}^0} \frac{d^3p'_2}{(2\pi)^3 2p'_2{}^0} (2\pi)^4 \delta^{(4)}(p'_1 + p'_2 + k - p_a - p_b) \\ \times \frac{1}{4} \sum_{p \text{ spins}} \mathcal{M}_\mu(p'_1, p'_2) (\mathcal{M}_\nu(p'_1, p'_2))^* (-g^{\mu\nu})$$

where $\sum_{\lambda_\gamma} (\epsilon^\mu)^* \epsilon^\nu = -g^{\mu\nu}$

Our diffractive photon-bremsstrahlung amplitude is

$$\mathcal{M}_\mu^{(\text{standard})} = \mathcal{M}_\mu^{(a)} + \mathcal{M}_\mu^{(b)} + \mathcal{M}_\mu^{(c)} + \mathcal{M}_\mu^{(d)} + \mathcal{M}_\mu^{(e)} + \mathcal{M}_\mu^{(f)}$$

The amplitude must satisfy the gauge-invariant relation $k^\mu \mathcal{M}_\mu^{(\text{standard})} = 0$

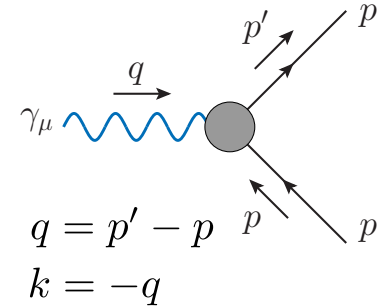
- We use the following standard proton propagator and γpp vertex:

$$iS_F(p) = \frac{i}{\not{p} - m_p + i\epsilon} = i \frac{\not{p} + m_p}{p^2 - m_p^2 + i\epsilon}$$

$$i\Gamma_\mu^{(\gamma pp)}(p', p) = -ie \left[F_1(0) \gamma_\mu + \frac{i}{2m_p} \sigma_{\mu\nu} q^\nu F_2(0) \right] \quad \leftarrow \text{form factors at } k^2 = 0$$

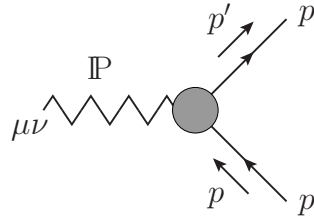
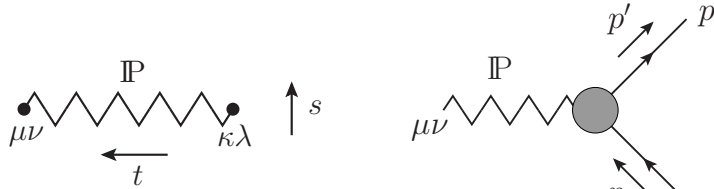
$$F_1(0) = 1, \quad F_2(0) = \kappa_p = 1.7928$$

- Ward-Takahashi identity: $(p' - p)^\mu \Gamma_\mu^{(\gamma pp)}(p', p) = -e [S_F^{-1}(p') - S_F^{-1}(p)]$



Formalism

- We work within the **tensor-pomeron model** for soft hadronic high-energy reactions, proposed by **Ewerz, Maniatis, Nachtmann, Ann. Phys. 342 (2014) 31**.
- This model has a good basis from nonperturbative QCD considerations; see **Nachtmann, Ann. Phys. 209 (1991) 436**.
- Tensor-pomeron model assumes that all $C = +1$ Regge exchanges (**pomeron IP**, f_2 and a_2 reggeons) are described as effective rank-2 symmetric tensor exchanges and the $C = -1$ exchanges (odderon, ω and ρ reggeons) as effective vector exchanges.
- Propagator for tensor-pomeron exchange and pomeron-proton vertex:



$$i\Delta_{\mu\nu,\kappa\lambda}^{(\mathbb{P})}(s, t) = \frac{1}{4s} \left(g_{\mu\kappa}g_{\nu\lambda} + g_{\mu\lambda}g_{\nu\kappa} - \frac{1}{2}g_{\mu\nu}g_{\kappa\lambda} \right) (-is\alpha'_{\mathbb{P}})^{\alpha_{\mathbb{P}}(t)-1}$$

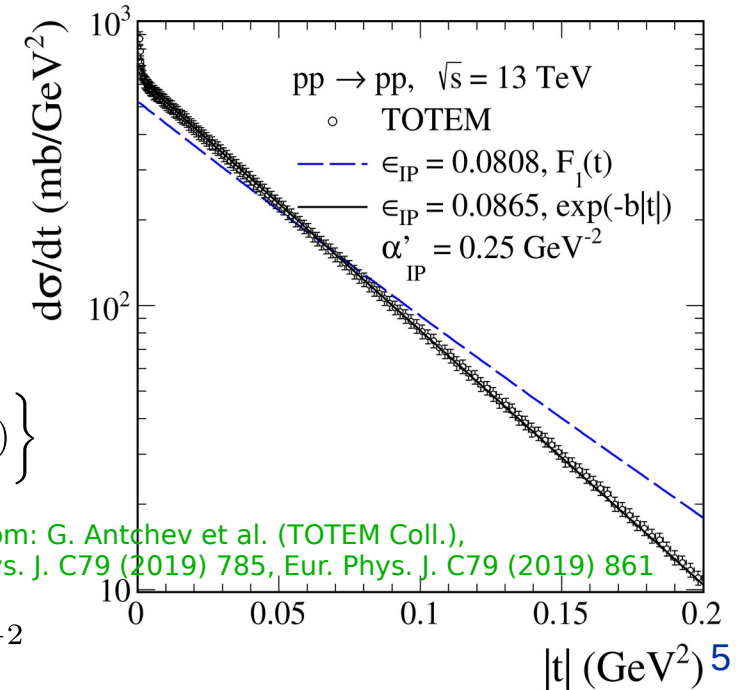
$$\alpha_{\mathbb{P}}(t) = \alpha_{\mathbb{P}}(0) + \alpha'_{\mathbb{P}}t, \quad \alpha_{\mathbb{P}}(0) = 1 + \epsilon_{\mathbb{P}} = 1.0808, \quad \alpha'_{\mathbb{P}} = 0.25 \text{ GeV}^{-2}$$

$$i\Gamma_{\mu\nu}^{(\mathbb{P}pp)}(p', p) = -i3\beta_{\mathbb{P}pp}F_1(t) \left\{ \frac{1}{2} [\gamma_{\mu}(p' + p)_{\nu} + \gamma_{\nu}(p' + p)_{\mu}] - \frac{1}{4}g_{\mu\nu}(\not{p}' + \not{p}) \right\}$$

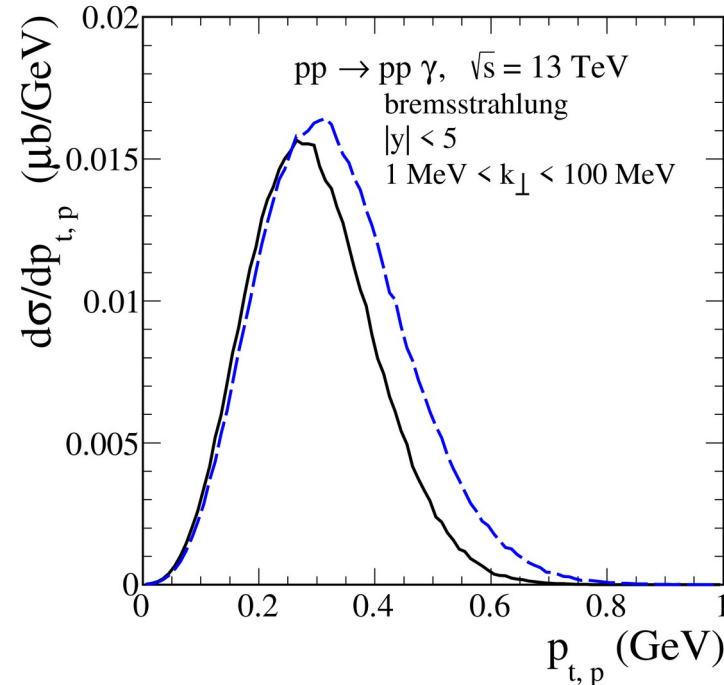
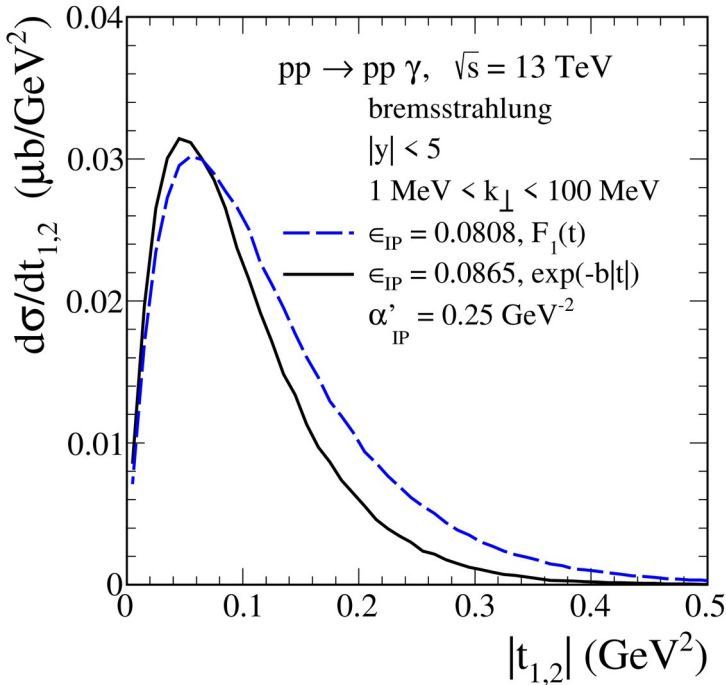
$$\beta_{\mathbb{P}pp} = 1.87 \text{ GeV}^{-1}$$

From comparison to the TOTEM $d\sigma/dt$ data:

$$\epsilon_{\mathbb{P}} = 0.0865 \quad F_1(t) \rightarrow F(t) = \exp(-b|t|) \quad \text{with } b = 2.95 \text{ GeV}^{-2}$$



Distributions in $|t|$ and $p_{t,p}$



- The distributions in four-momentum transfer squared $|t_{1,2}|$ where $t_{1,2}$ is either t_1 or t_2 and in transverse momentum of the outgoing proton $p_{t,p}$
- Photons come predominantly from pp collisions with momentum transfers between the protons of order $p_{t,p} \sim \sqrt{|t_{1,2}|} \sim 0.3 \text{ GeV}$

Formalism

- The kinematic variables for the $pp \rightarrow ppy$ reaction are:

$$s = (p_a + p_b)^2 = (p'_1 + p'_2 + k)^2$$

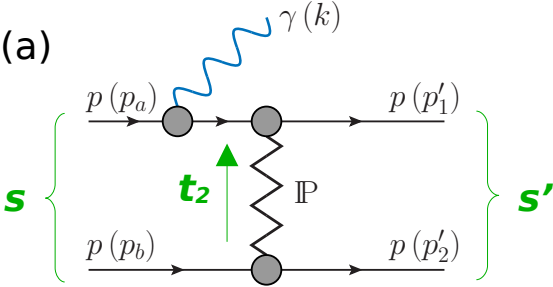
$$s' = (p_a + p_b - k)^2 = (p'_1 + p'_2)^2$$

$$t_1 = (p_a - p'_1)^2 = (p_b - p'_2 - k)^2$$

$$t_2 = (p_b - p'_2)^2 = (p_a - p'_1 - k)^2$$

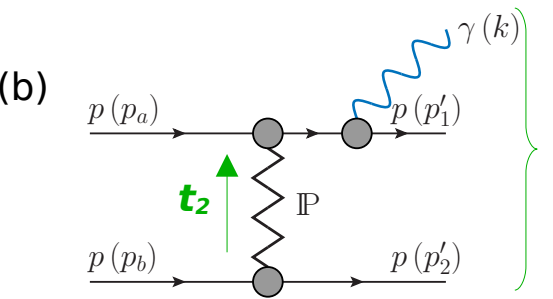
$$\mathcal{F}_{\mathbb{P}}(s, t) = [3\beta_{\mathbb{P}pp}F(t)]^2 \frac{1}{4s} (-is\alpha'_{\mathbb{P}})^{\alpha_{\mathbb{P}}(t)-1}$$

- We get with the **off-shell scattering amplitudes** (with only IP exchange) for diagrams (a) and (b):

(a)  $\mathcal{M}_{\mu}^{(a)} = -\bar{u}_{1'} \otimes \bar{u}_{2'} \mathcal{M}^{(0)}(p_a - k, p_b, p'_1, p'_2) [S_F(p_a - k) \Gamma_{\mu}^{(\gamma pp)}(p_a - k, p_a) u_a] \otimes u_b$

$$= e \bar{u}_{1'} \otimes \bar{u}_{2'} \{ i \mathcal{F}_{\mathbb{P}}(s', t_2) [\gamma^{\alpha} \otimes \gamma_{\alpha} (p_a - k + p'_1, p_b + p'_2) + (\not{p}_b + \not{p}'_2) \otimes (\not{p}_a - \not{k} + \not{p}'_1) - \frac{1}{2} (\not{p}_a - \not{k} + \not{p}'_1) \otimes (\not{p}_b + \not{p}'_2)] \}$$

$$\times \left[\frac{\not{p}_a - \not{k} + m_p}{(p_a - k)^2 - m_p^2 + i\varepsilon} \left(\gamma_{\mu} - \frac{i}{2m_p} \sigma_{\mu\nu} k^{\nu} F_2(0) \right) u_a \right] \otimes u_b$$

(b)  $\mathcal{M}_{\mu}^{(b)} = -[\bar{u}_{1'} \Gamma_{\mu}^{(\gamma pp)}(p'_1, p'_1 + k) S_F(p'_1 + k)] \otimes \bar{u}_{2'} \mathcal{M}^{(0)}(p_a, p_b, p'_1 + k, p'_2) u_a \otimes u_b$

$$= e [\bar{u}_{1'} \left(\gamma_{\mu} - \frac{i}{2m_p} \sigma_{\mu\nu} k^{\nu} F_2(0) \right) \frac{\not{p}'_1 + \not{k} + m_p}{(p'_1 + k)^2 - m_p^2 + i\varepsilon}] \otimes \bar{u}_{2'}$$

$$\times \{ i \mathcal{F}_{\mathbb{P}}(s, t_2) [\gamma^{\alpha} \otimes \gamma_{\alpha} (p_a + p'_1 + k, p_b + p'_2) + (\not{p}_b + \not{p}'_2) \otimes (\not{p}_a + \not{p}'_1 + \not{k}) - \frac{1}{2} (\not{p}_a + \not{p}'_1 + \not{k}) \otimes (\not{p}_b + \not{p}'_2)] \} u_a \otimes u_b$$

Formalism

Using the Ward-Takahashi identity we find

$$\begin{aligned} k^\mu \mathcal{M}_\mu^{(a)} &= -e \bar{u}_{1'} \otimes \bar{u}_{2'} \mathcal{M}^{(0)}(p_a - k, p_b, p'_1, p'_2) u_a \otimes u_b, \\ k^\mu \mathcal{M}_\mu^{(b)} &= e \bar{u}_{1'} \otimes \bar{u}_{2'} \mathcal{M}^{(0)}(p_a, p_b, p'_1 + k, p'_2) u_a \otimes u_b. \end{aligned}$$

Now we impose the gauge invariance condition which must hold also for the photon emission from the p_a - p'_1 lines in (a – c) diagrams alone:

$$k^\mu (\mathcal{M}_\mu^{(a)} + \mathcal{M}_\mu^{(b)} + \mathcal{M}_\mu^{(c)}) = 0.$$

We obtain then:

$$\begin{aligned} k^\mu \mathcal{M}_\mu^{(c)} &= -k^\mu \mathcal{M}_\mu^{(a)} - k^\mu \mathcal{M}_\mu^{(b)} \\ &= e \bar{u}_{1'} \otimes \bar{u}_{2'} [\mathcal{M}^{(0)}(p_a - k, p_b, p'_1, p'_2) - \mathcal{M}^{(0)}(p_a, p_b, p'_1 + k, p'_2)] u_a \otimes u_b \end{aligned}$$

The explicit expressions of the amplitudes are given in [Lebiedowicz, Nachtmann, Szczurek, PRD 106 \(2022\) 034023](#)

We rewrite the amplitude in a way that is more suitable for numerical computations:

$$\begin{aligned} \mathcal{M}_\mu^{(\text{standard})} &= \mathcal{M}_\mu^{(a)} + \mathcal{M}_\mu^{(b)} + \mathcal{M}_\mu^{(c)} + \mathcal{M}_\mu^{(d)} + \mathcal{M}_\mu^{(e)} + \mathcal{M}_\mu^{(f)} \\ &= \sum_{j=1}^7 (\mathcal{M}_\mu^{(a+b+c)j} + \mathcal{M}_\mu^{(d+e+f)j}) \quad \text{all subamplitudes (a+b+c) and (d+e+f)} \\ &\quad \text{are separately gauge invariant} \end{aligned}$$

Formalism

For $j = 1, 2, 4$ we have

$$\mathcal{M}_\mu^{(a+b+c)1} = e\bar{u}_{1'} \otimes \bar{u}_{2'} \left\{ i\mathcal{F}_\mathbb{P}(s, t_2) [\gamma^\alpha \otimes \gamma_\alpha(p_a + p'_1, p_b + p'_2) + (\not{p}_b + \not{p}'_2) \otimes (\not{p}_a + \not{p}'_1) - 2m_p^2 1 \otimes 1] \right. \\ \left. \times \left[\frac{2p_{a\mu} - k_\mu}{-2p_a \cdot k + k^2 + i\varepsilon} + \frac{2p'_{1\mu} + k_\mu}{2p'_1 \cdot k + k^2 + i\varepsilon} \right] \right\} u_a \otimes u_b$$

← the subamplitude $j = 1$ contains the pole term $\propto 1/\omega$ for $\omega \rightarrow 0$

$$\mathcal{M}_\mu^{(a+b+c)2} = e\bar{u}_{1'} \otimes \bar{u}_{2'} \left\{ i\mathcal{F}_\mathbb{P}(s', t_2) \frac{1}{-2p_a \cdot k + k^2 + i\varepsilon} \right. \\ \times [\gamma^\alpha \otimes \gamma_\alpha(p_a + p'_1 - k, p_b + p'_2) + (\not{p}_b + \not{p}'_2) \otimes (\not{p}_a + \not{p}'_1 - \not{k})] \\ \left. \times \left[k_\mu - \not{k}\gamma_\mu + \frac{F_2(0)}{2m_p} (2p_{a\mu} \not{k} - 2(p_a \cdot k)\gamma_\mu + 2m_p(k_\mu - \not{k}\gamma_\mu) - (\not{k}k_\mu - k^2\gamma_\mu)) \right] \otimes 1 \right\} u_a \otimes u_b$$

ω is the energy of the photon

$$\mathcal{M}_\mu^{(a+b+c)4} = e\bar{u}_{1'} \otimes \bar{u}_{2'} \left\{ i\mathcal{F}_\mathbb{P}(s, t_2) \frac{1}{2p'_1 \cdot k + k^2 + i\varepsilon} \right. \\ \times \left[- (k_\mu - \gamma_\mu \not{k}) + \frac{F_2(0)}{2m_p} (-2p'_{1\mu} \not{k} + 2(p'_1 \cdot k)\gamma_\mu - 2m_p(k_\mu - \gamma_\mu \not{k}) - (k_\mu \not{k} - k^2\gamma_\mu)) \right] \otimes 1 \\ \left. \times [\gamma^\alpha \otimes \gamma_\alpha(p_a + p'_1 + k, p_b + p'_2) + (\not{p}_b + \not{p}'_2) \otimes (\not{p}_a + \not{p}'_1 + \not{k})] \right\} u_a \otimes u_b$$

Here $\mathcal{F}_\mathbb{P}(s, t) = [3\beta_{\mathbb{P}pp}F(t)]^2 \frac{1}{4s} (-is\alpha'_\mathbb{P})^{\alpha_\mathbb{P}(t)-1}$

The terms $j = 2$ and 4 have no singularity for $\omega \rightarrow 0$.

The main term there comes from the anomalous magnetic moment $F_2(0)$.

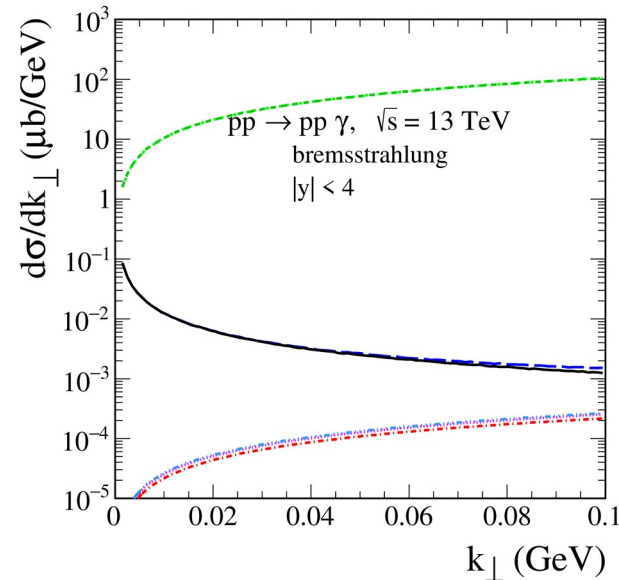
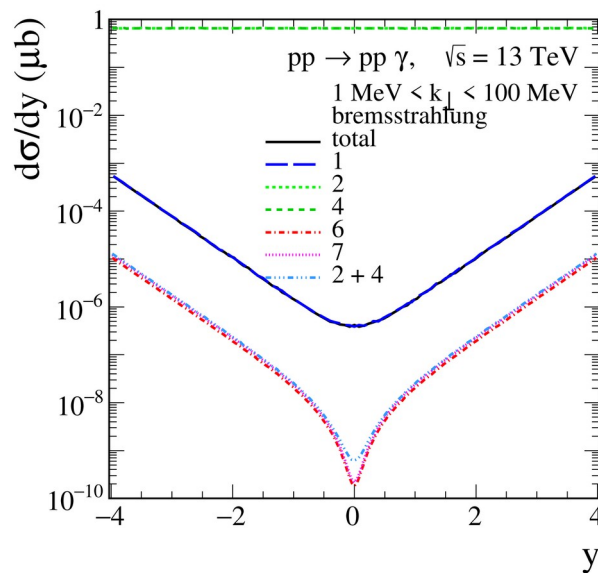
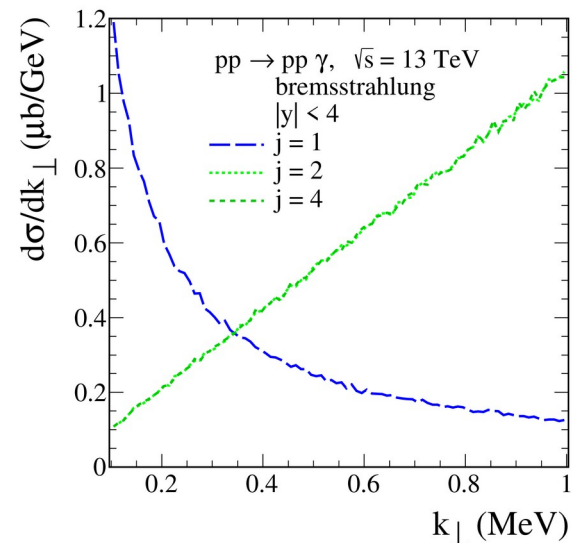
- We show the complete result (total) including interference effects and the results for individual j terms, except for $j = 3$ and 5 which are very small and can be neglected. The coherent sum of the amplitudes with $j = 2$ and 4 is denoted by $2 + 4$.

- There is significant cancellation among the terms $j = 2$ and 4 due to destructive interference (not due to a gauge cancellation) and their sum is harmless, well below the term $j = 1$, at least for $k_{\perp} < 100$ MeV.

This leads to a much larger region in k_{\perp} and ω where the pole term gives a good representation of the radiative amplitude.

- It is essential to add coherently all the various parts of the amplitude for soft photon emission in order not to miss important interference effects!

The pole term ($j = 1$) has singularity for $k_{\perp} \rightarrow 0$. Thus, the term $j = 1$ will win over $j=2, 4$ terms individually for $\omega \rightarrow 0$.



Formalism

- We compare our standard (exact) results to two **soft-photon approximations**, SPA1 and SPA2, where we keep in the radiative amplitudes **only the pole terms proportional to $1/\omega$** :

– SPA1

$$\mathcal{M}_{\mu, \text{SPA1}} = e \mathcal{M}^{(\text{on shell}) pp}(s, t) \left[-\frac{p_{a\mu}}{(p_a \cdot k)} + \frac{p_{1\mu}}{(p_1 \cdot k)} - \frac{p_{b\mu}}{(p_b \cdot k)} + \frac{p_{2\mu}}{(p_2 \cdot k)} \right]$$

$$\begin{aligned} d\sigma(pp \rightarrow pp\gamma)_{\text{SPA1}} &= \frac{d^3k}{(2\pi)^3 2k^0} \int d^3p_1 d^3p_2 e^2 \frac{d\sigma(pp \rightarrow pp)}{d^3p_1 d^3p_2} \\ &\times \left[-\frac{p_{a\mu}}{(p_a \cdot k)} + \frac{p_{1\mu}}{(p_1 \cdot k)} - \frac{p_{b\mu}}{(p_b \cdot k)} + \frac{p_{2\mu}}{(p_2 \cdot k)} \right] \left[-\frac{p_{a\nu}}{(p_a \cdot k)} + \frac{p_{1\nu}}{(p_1 \cdot k)} - \frac{p_{b\nu}}{(p_b \cdot k)} + \frac{p_{2\nu}}{(p_2 \cdot k)} \right] (-g^{\mu\nu}) \\ \frac{d\sigma(pp \rightarrow pp)}{d^3p_1 d^3p_2} &= \frac{1}{2\sqrt{s(s-4m_p^2)}} \frac{1}{(2\pi)^3 2p_1^0 (2\pi)^3 2p_2^0} (2\pi)^4 \delta^{(4)}(p_1 + p_2 - p_a - p_b) \frac{1}{4} \sum_{p \text{ spins}} |\mathcal{M}^{(\text{on shell}) pp}(s, t)|^2 \end{aligned}$$

in high-energy small-angle limit



$$\begin{aligned} \mathcal{M}(s, t) &\approx i8s^2 \mathcal{F}_{\mathbb{P}pp}(s, t) \delta_{\lambda_1 \lambda_a} \delta_{\lambda_2 \lambda_b} \\ &\approx i2s [3\beta_{\mathbb{P}pp} F(t)]^2 (-is\alpha'_{\mathbb{P}})^{\alpha_{\mathbb{P}}(t)-1} \delta_{\lambda_1 \lambda_a} \delta_{\lambda_2 \lambda_b} \end{aligned}$$

– SPA2

$$\mathcal{M}_{\mu, \text{SPA2}} = \mathcal{M}_{\mu}^{(a+b+c)1}(s, t_2) + \mathcal{M}_{\mu}^{(d+e+f)1}(s, t_1)$$

Comparison of our “exact” model or “standard” bremsstrahlung results with SPAs

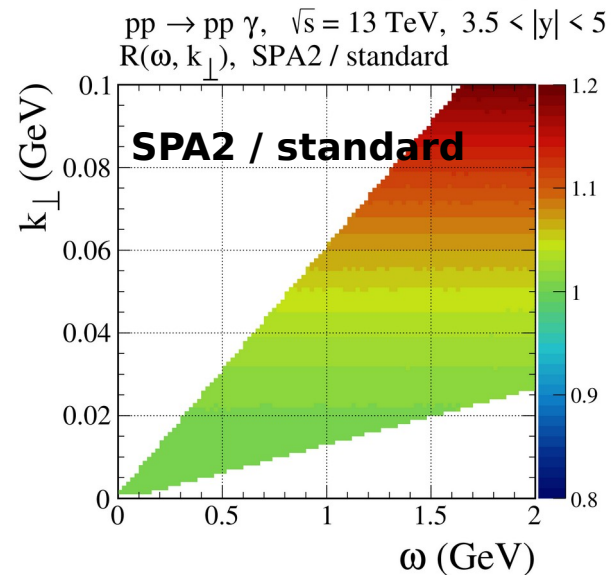
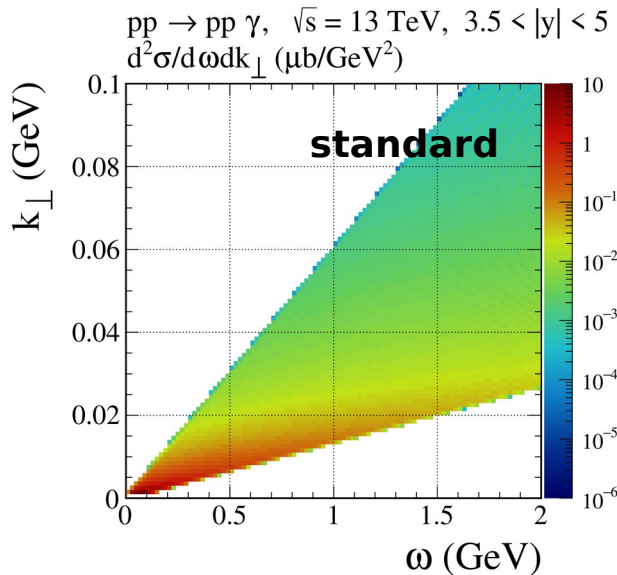
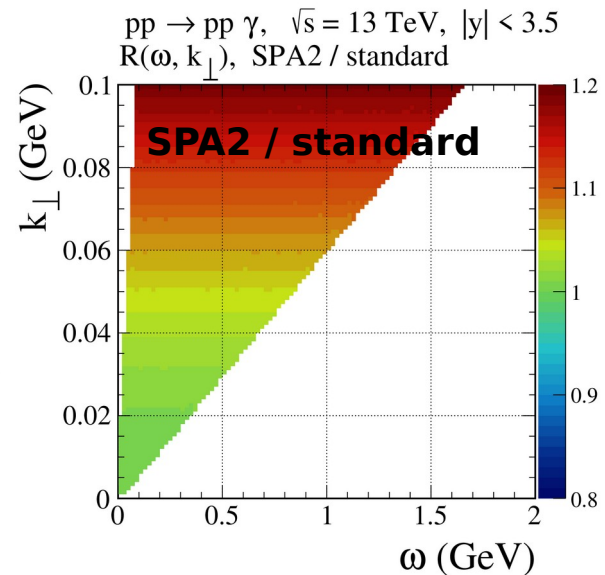
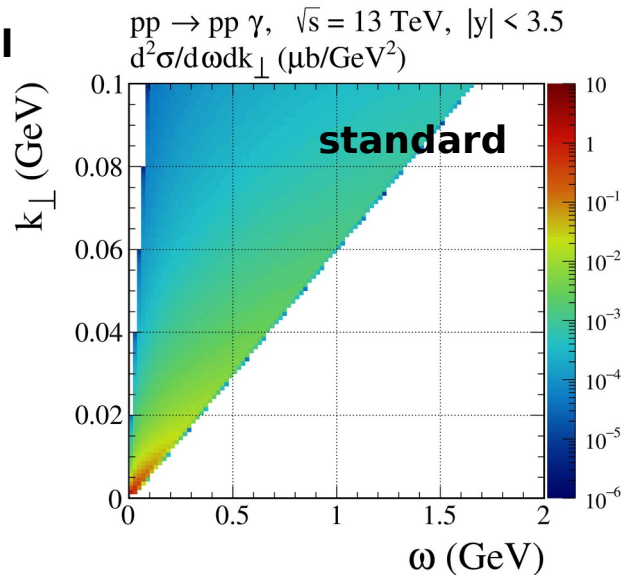
- In the left panels we show two-dimensional differential cross sections in the ω - k_{\perp} plane.

Large y is near the ω axis, and $y = 0$ corresponds to the line $\omega = k_{\perp}$, both in accordance with $\omega = k_{\perp} \cosh y$.

- In the right panels we show the ratio

$$R(\omega, k_{\perp}) = \frac{d^2\sigma_{\text{SPA2}}/d\omega dk_{\perp}}{d^2\sigma_{\text{standard}}/d\omega dk_{\perp}}$$

One can see that SPA2 stays within 1% accuracy for $k_{\perp} < 22$ MeV and $\omega < 0.35$ GeV considering $|y| < 3.5$ and up to $\omega \approx 1.7$ GeV for $3.5 < |y| < 5.0$.

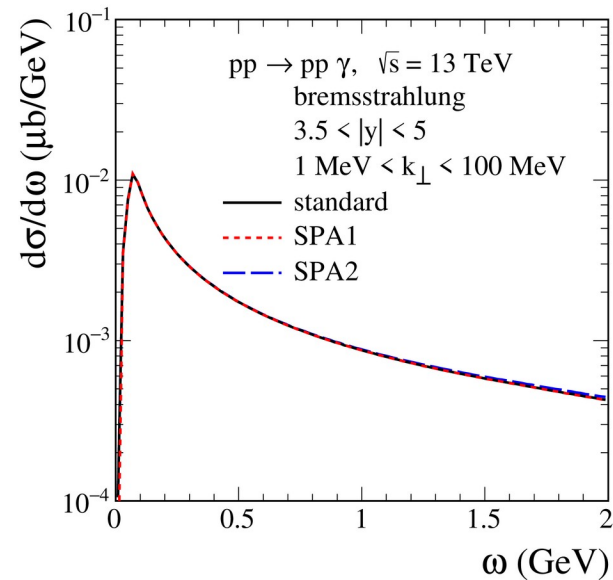
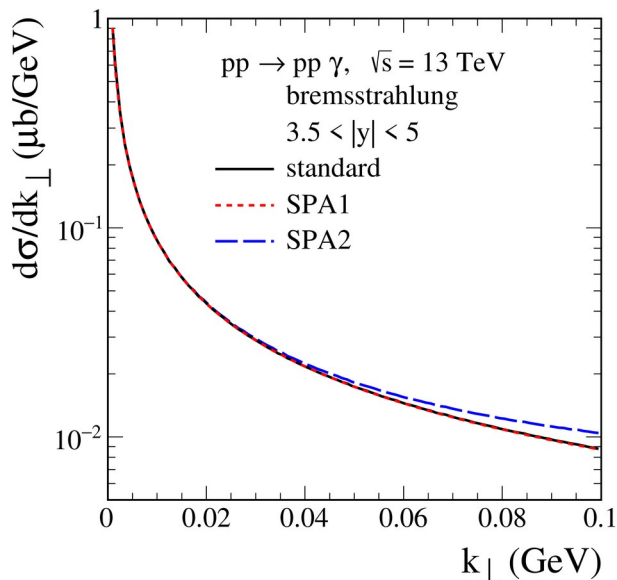


Comparison of “standard” results to SPA 1 and SPA 2

- (top panels)
Both SPAs follow the standard results very well.

Where the $1/\omega$ term gives a reliable result?

Surprisingly, the SPA 1 which does not have the correct energy-momentum relations fares somewhat better than SPA2.



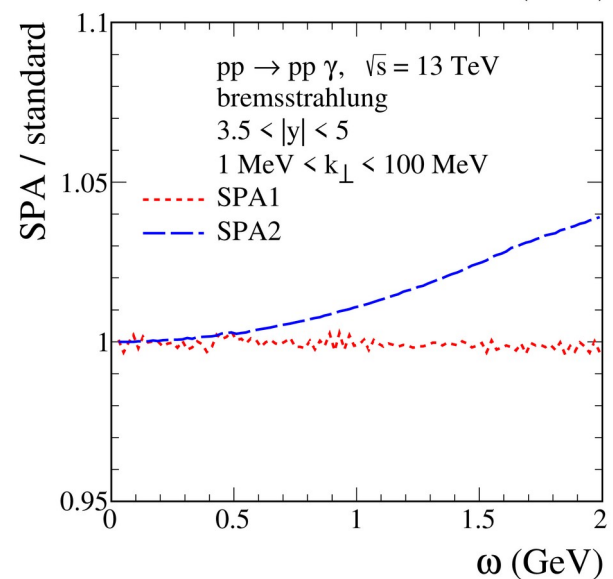
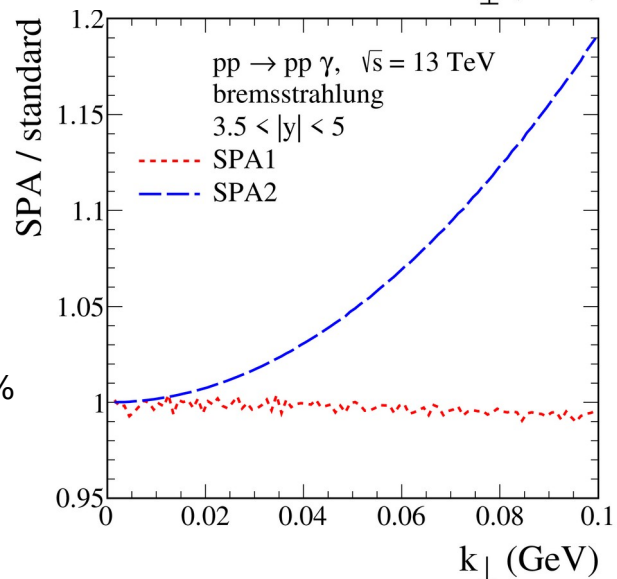
- (bottom panels)
We show the ratios of the SPAs to the standard cross sections:

$$\frac{d\sigma_{\text{SPA}}/dk_{\perp}}{d\sigma_{\text{standard}}/dk_{\perp}} \quad \text{and} \quad \frac{d\sigma_{\text{SPA}}/d\omega}{d\sigma_{\text{standard}}/d\omega}$$

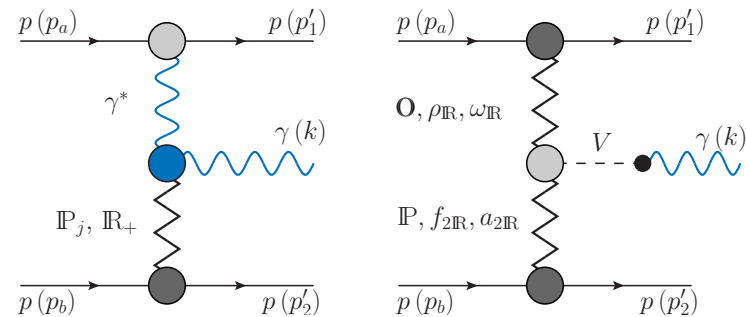
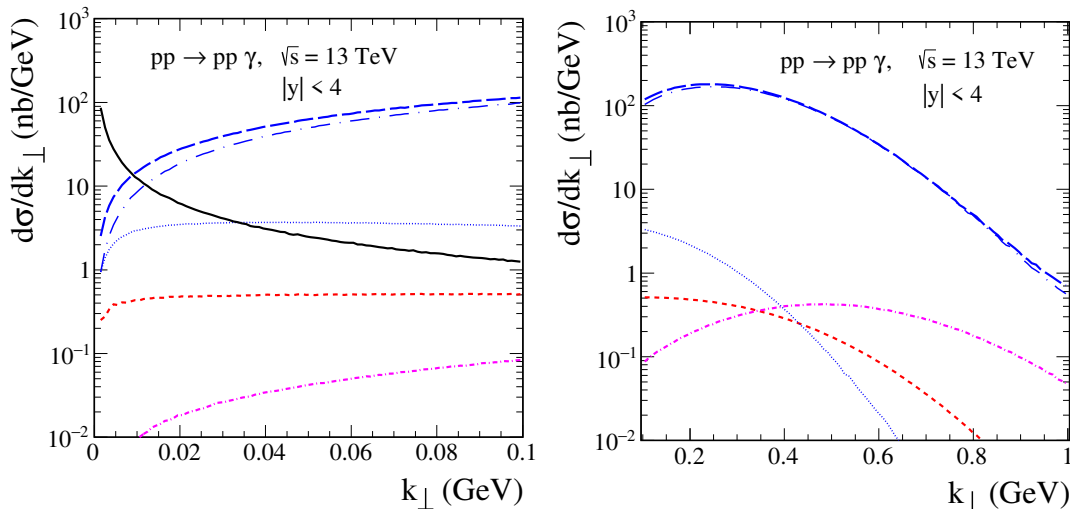
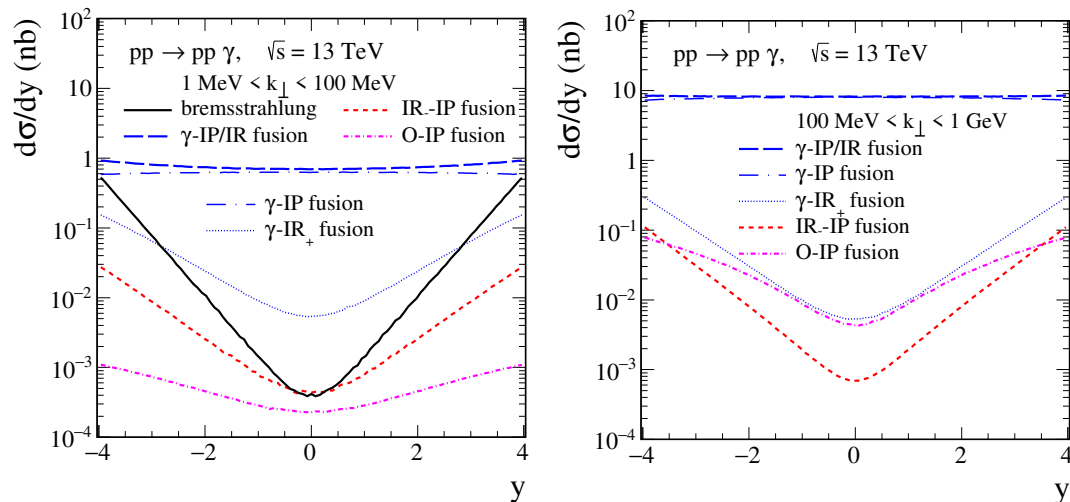
as function of k_{\perp} and ω , respectively.

One can see that the deviations of the SPA1 from the standard results are up to around 1% in considered region.

For the SPA2 the deviations increase rapidly with growing k_{\perp} and ω .



Results, CEP vs diff. bremsstrahlung

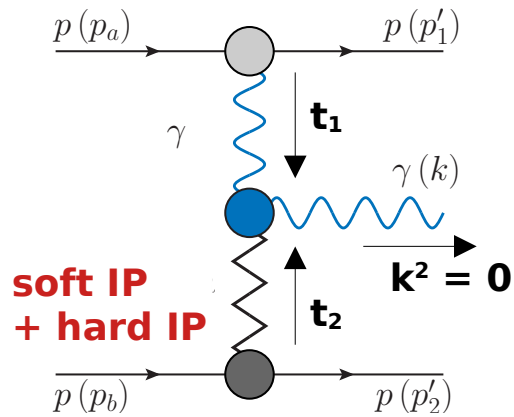


PRD 107 (2023) 074014

At midrapidities, the photoproduction (left diagram) gives a much larger cross section than bremsstrahlung.

The soft-photon bremsstrahlung is important in the forward rapidity range, $|y| > 4$, and at very small k_{\perp} .

CEP via γ^* - IP/IR fusion is intimately related to DVCS (PLB 835 (2022) 137497).



The Ansatz for the **IP** $\gamma\gamma$ coupling functions for both real and virtual photons is discussed in [Britzger, Ewerz, Glazov, Nachtmann, Schmitt, PRD 100 \(2019\) 114007](#).

The coupling functions \hat{a} and \hat{b} were determined from the global fit to HERA inclusive DIS data and the total photoproduction cross section $\sigma_{\gamma p}$, and from HERA DVCS data.

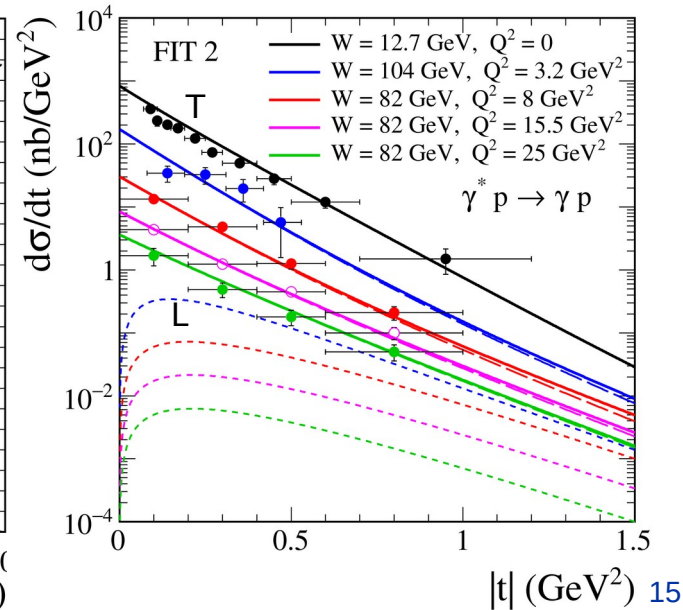
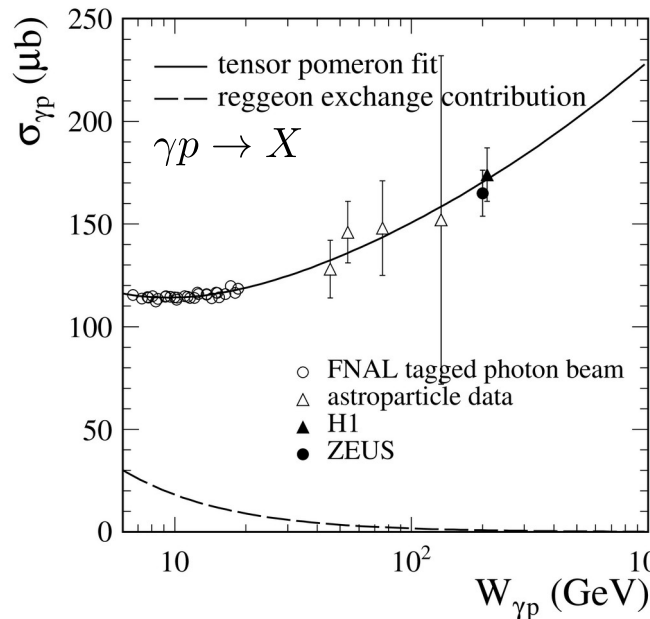
The t dependence of γp subsystem is from fit of the model to the FNAL data on real Compton scattering $\gamma p \rightarrow \gamma p$ (and also to DVCS HERA data)

$$\begin{aligned} F_{\text{eff}}^{(\mathbb{P})}(t) &= F^{(\mathbb{P}\gamma\gamma)}(t) \times F^{(\mathbb{P}pp)}(t) \\ &= \exp(-b_{\text{eff}}|t|/2) \end{aligned}$$

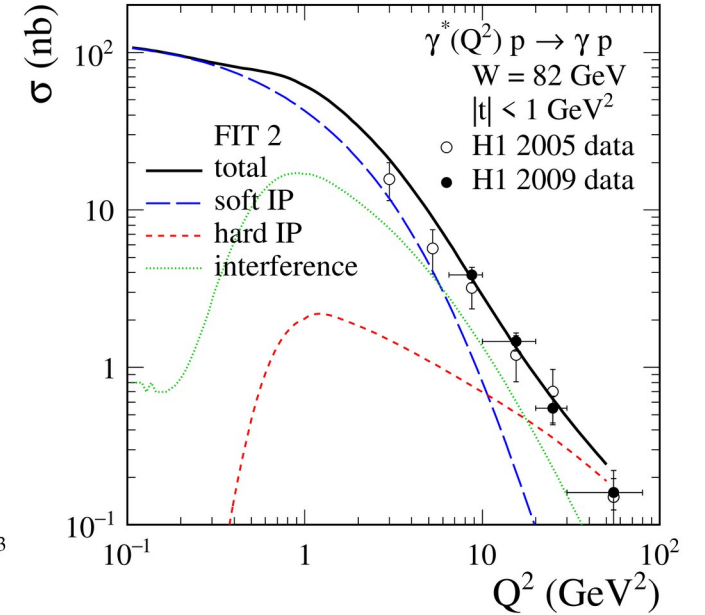
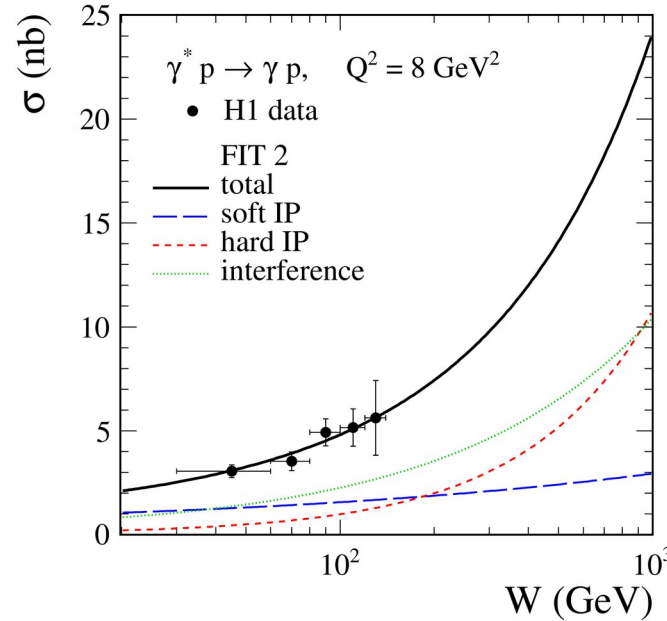
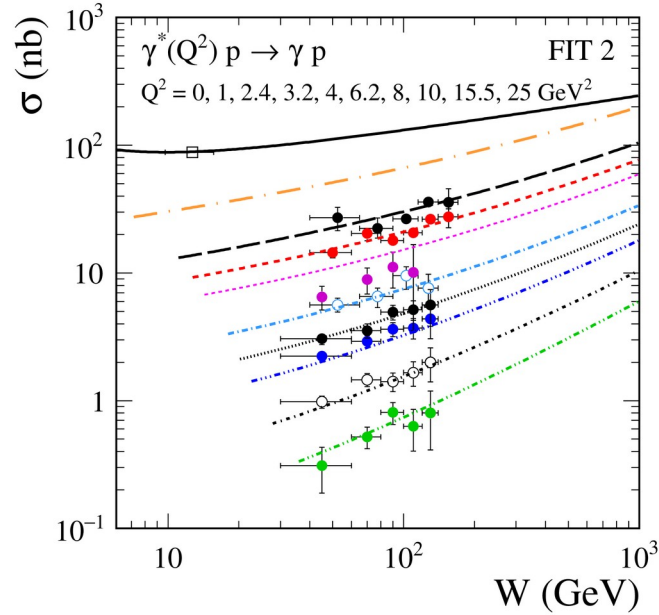
The $\gamma\mathbb{P}$ -exchange amplitude can be written as

$$\begin{aligned} \mathcal{M}_{\mu}^{(\gamma\mathbb{P})} &= (-i) \bar{u}_1 i \Gamma_{\nu_1}^{(\gamma pp)}(p'_1, p_a) u_a i \Delta^{(\gamma)} \nu_1 \nu(q_1) i \Gamma_{\mu\nu\kappa\rho}^{(\mathbb{P}\gamma^*\gamma)}(k, q_1) i \Delta^{(\mathbb{P})} \kappa\rho, \alpha\beta(s_2, t_2) \\ &\quad \times \bar{u}_{2'} i \Gamma_{\alpha\beta}^{(\mathbb{P}pp)}(p'_2, p_b) u_b \\ &= \bar{u}_1 \Gamma^{(\gamma pp)} \nu(p'_1, p_a) u_a \frac{1}{t_1} \frac{1}{2s_2} (-is_2 \alpha'_{\mathbb{P}})^{\alpha\mathbb{P}(t_2)-1} \bar{u}_{2'} \Gamma_{\alpha\beta}^{(\mathbb{P}pp)}(p'_2, p_b) u_b \\ &\quad \times i \left[2a_{\mathbb{P}\gamma^*\gamma}(t_1, k^2, t_2) \Gamma_{\mu\nu}^{(0)\alpha\beta}(k, -q_1) - b_{\mathbb{P}\gamma^*\gamma}(t_1, k^2, t_2) \Gamma_{\mu\nu}^{(2)\alpha\beta}(k, -q_1) \right] \end{aligned}$$

dominant term: $b_{\mathbb{P}\gamma^*\gamma}(-Q_1^2, 0, t_2) = e^2 \hat{b}_{\mathbb{P}}(Q_1^2) F^{(\mathbb{P}\gamma\gamma)}(t_2)$
where $Q_1^2 = -t_1$ is the photon virtuality

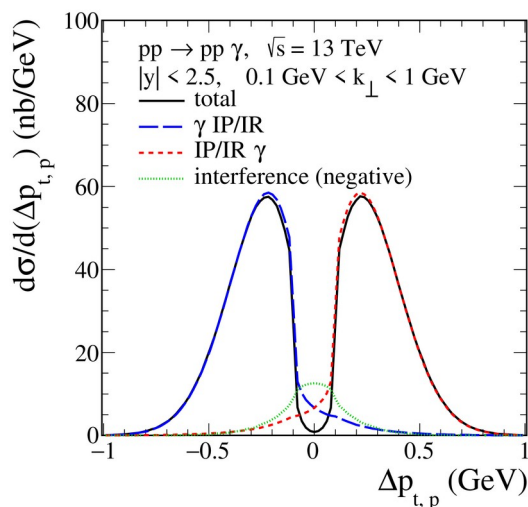
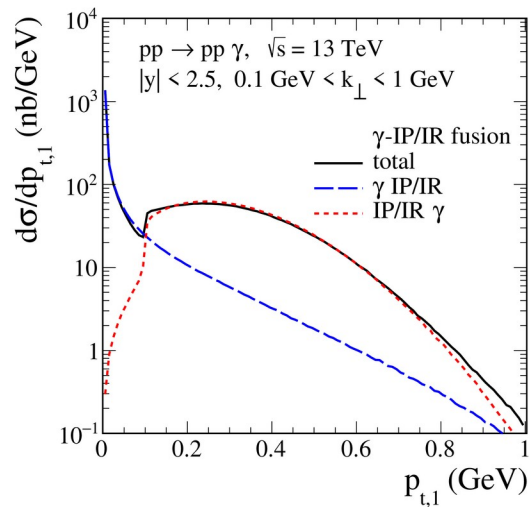


- **Comparison of two-tensor pomeron model with DVCS data**



- This Regge type model can be used for large energy W , $|t| \lesssim 1 \text{ GeV}^2$, and small Bjorken- x , say $x \approx Q^2 / W^2 < 0.02$
- For real Compton scattering ($Q^2 = 0$) the cross section is dominated by soft-pomeron exchange with an additional contribution from reggeon exchange at lower energies W .
- For higher W , the contribution from the hard pomeron is enhanced, gives a steeper rise of the cross section with W ($\sigma \propto W^{2\epsilon}$, $\epsilon_{\text{softIP}} \approx 0.09 < \epsilon_{\text{hardIP}} \approx 0.3$) and especially so for larger Q^2 .
- For higher Q^2 the soft component slowly decreases relative to the hard one.
 A significant constructive interference effect between soft and hard components is clearly visible.

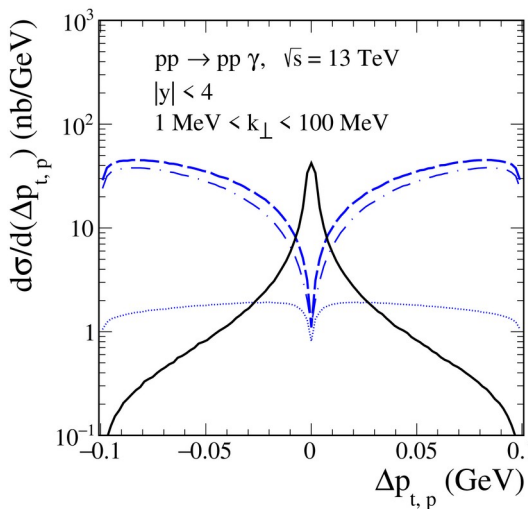
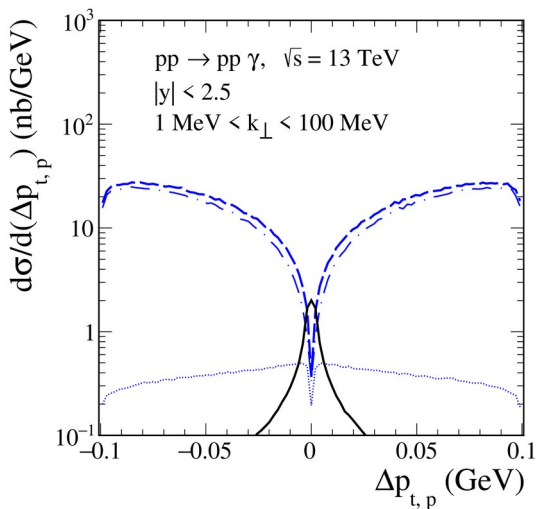
Results, $pp \rightarrow ppy$ (photoproduction)



In the CEP process (photoproduction) we have either $p_{t,1} \sim 0$, $p_{t,2}$ sizeable, or $p_{t,2} \sim 0$, $p_{t,1}$ sizeable.

This explains the double-hump structure in

$$\Delta p_{t,p} = |\mathbf{p}_{t,1}| - |\mathbf{p}_{t,2}|$$

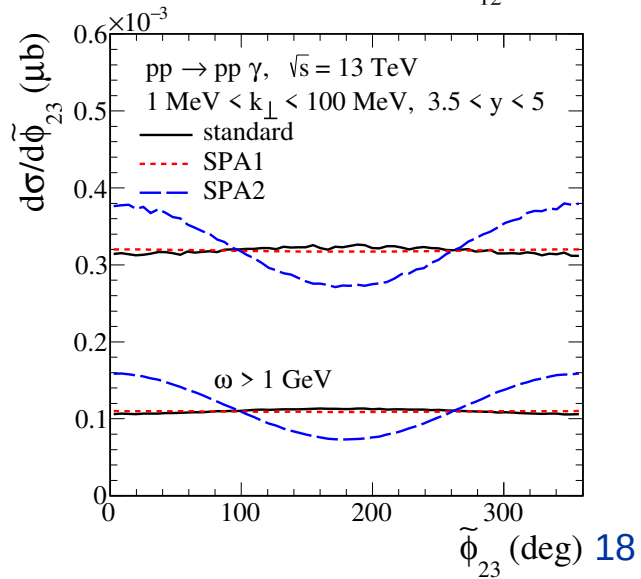
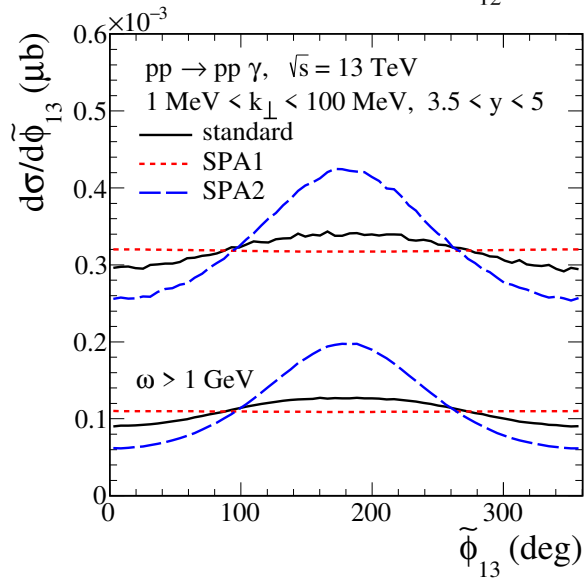
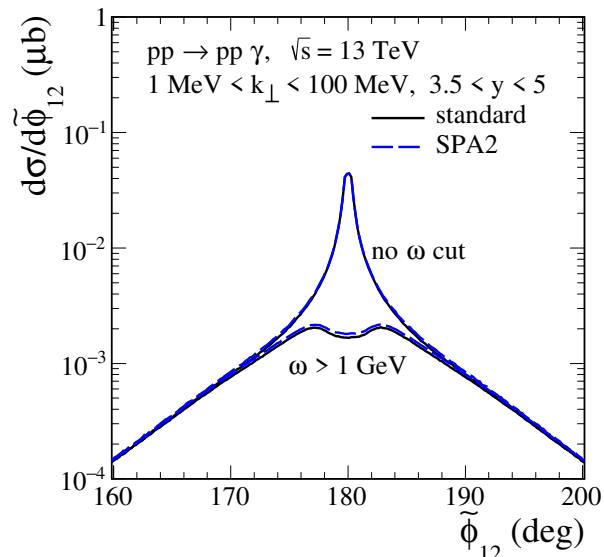
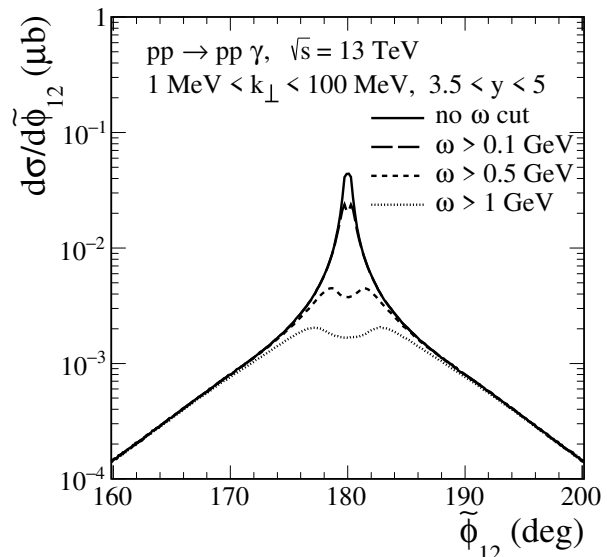


For bremsstrahlung, on the other hand, the kinematics of the $pp \rightarrow ppy$ reaction is close to that for elastic scattering ($pp \rightarrow pp$) where $p_{t,1} = p_{t,2}$.

We expect, therefore, also for bremsstrahlung $p_{t,1} \sim p_{t,2}$ and, thus, $\Delta p_{t,p} \sim 0$.

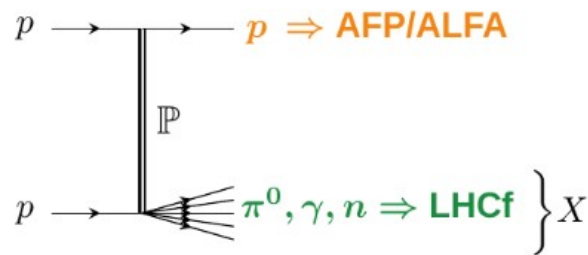
Results

- Predictions for the planned **ALICE 3** detector at the LHC
- The width of the distribution in $\tilde{\phi}_{12}$ depends on the ω cut
- For detailed comparisons of our predictions with experiment and in order to distinguish our standard and the approximate approaches (SPAs) measurement of the outgoing protons would be welcome

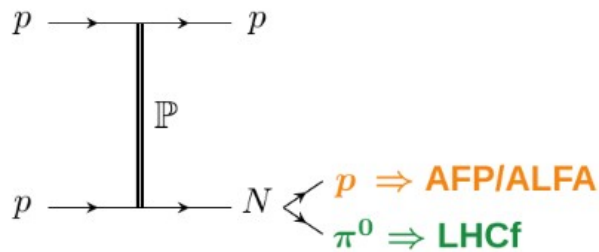


Introduction

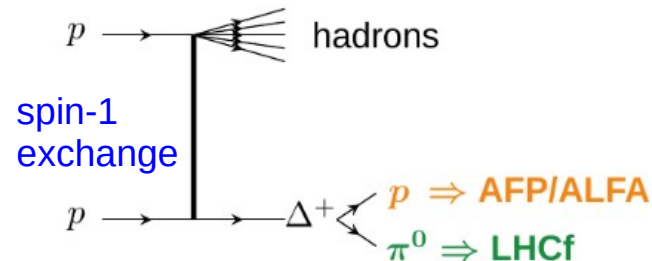
- ATLAS-LHCf analysis, *ATLAS PUB Note: Physics potential of a combined data taking of the LHCf and ATLAS Roman Pot detectors*, ATL-PHYS-PUB-2023-024



single diffraction



e.g. N(1440) excitation



In single diffractive dissociation events, one proton stays intact and is scattered at a small angle via a pomeron exchange (and could be detected by Roman Pot detectors) while the other one breaks up producing hadrons, of which a neutron, neutral pion or photon from a neutral meson decay can be detected by LHCf. In other cases, at least one of the protons enters an excited state during the collision with a subsequent decay into a $p\pi^0$ state.

The production of excitation states of the proton in soft QCD interactions has not been measured yet at the LHC.

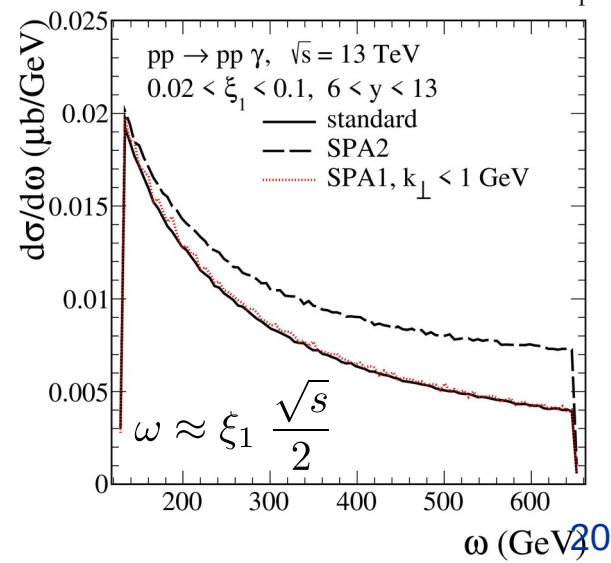
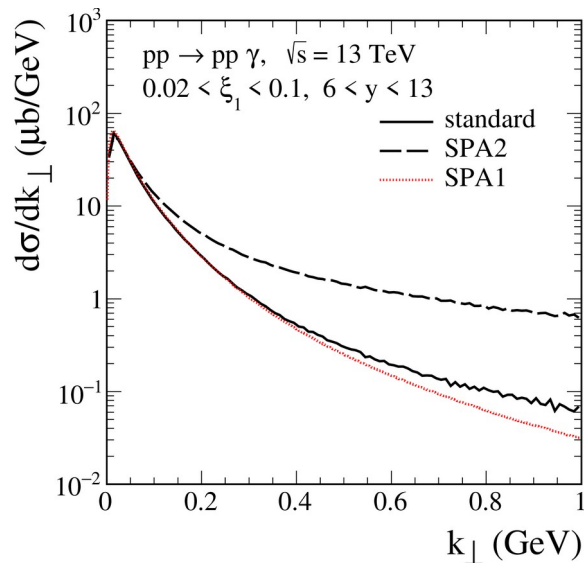
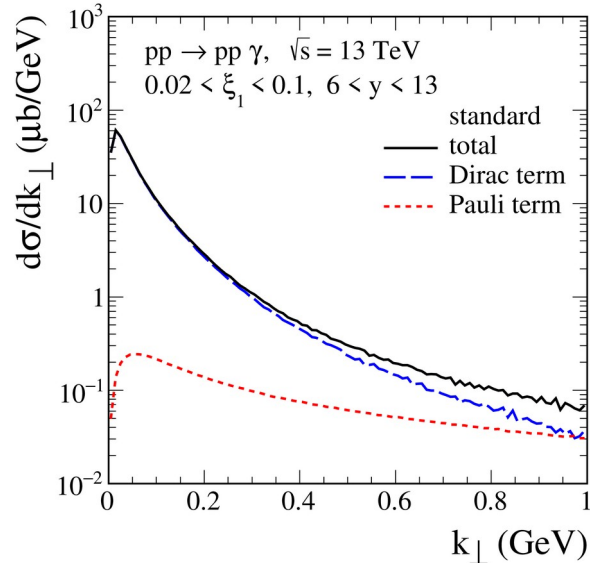
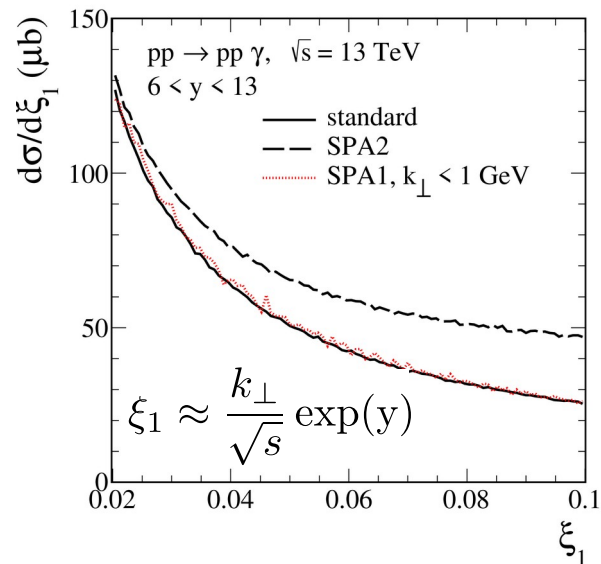
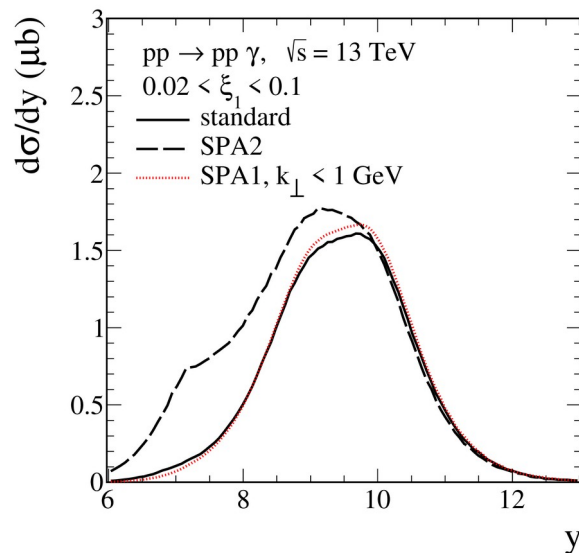
- In [Lebiedowicz, Nachtmann, Szczurek, PLB 843 \(2023\) 138053](#) we have discussed a possibility to measure exclusive diffractive bremsstrahlung of one and two photons in pp collisions with ATLAS-LHCf detectors.

Results, $pp \rightarrow pp\gamma$

In the forward-rapidity region (LHCf)
and for **proton relative energy loss**
 $0.02 < \xi_1 < 0.1$

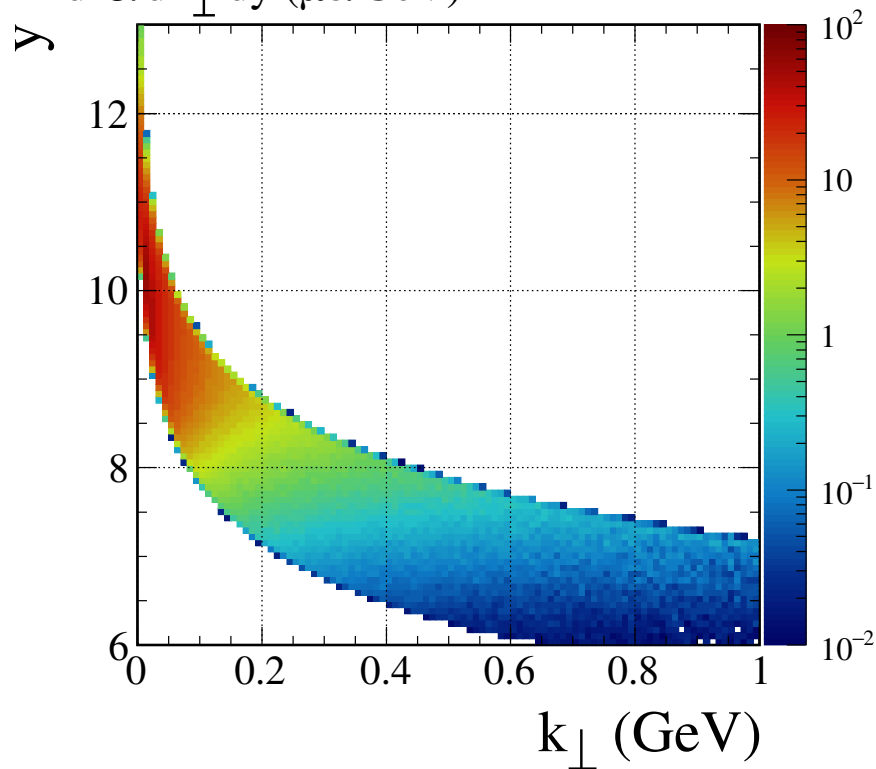
(ATLAS Roman Pot detectors, AFP)
our standard (exact) and SPA1 results are
very close to each other.

This is also the kinematic region where
soft-photon theorem should be applicable
($k_\perp < 0.2$ GeV).

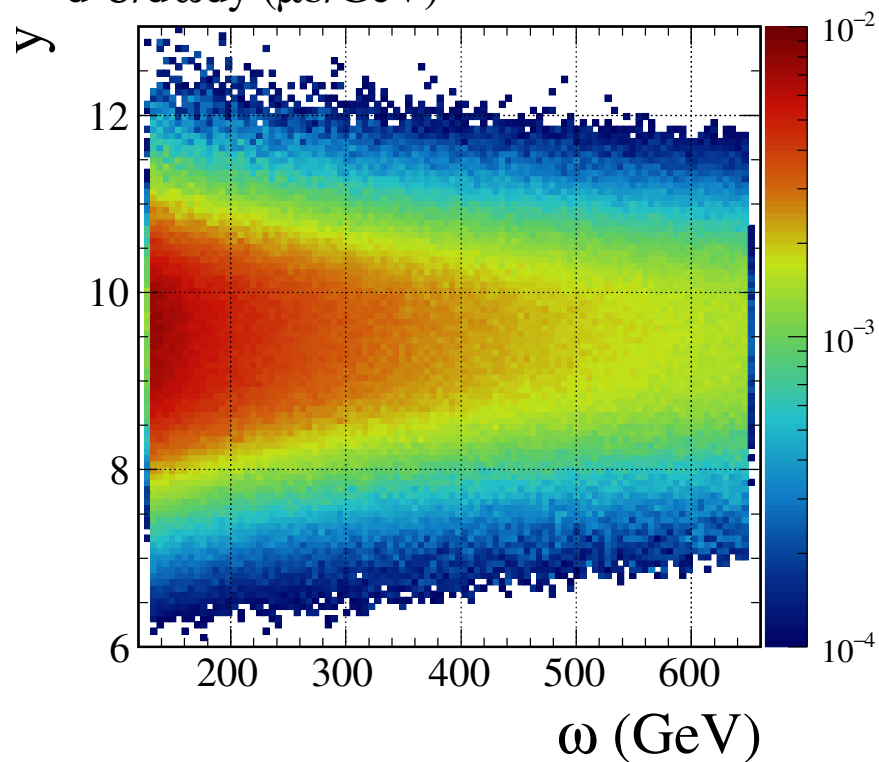


Results, $pp \rightarrow pp\gamma$

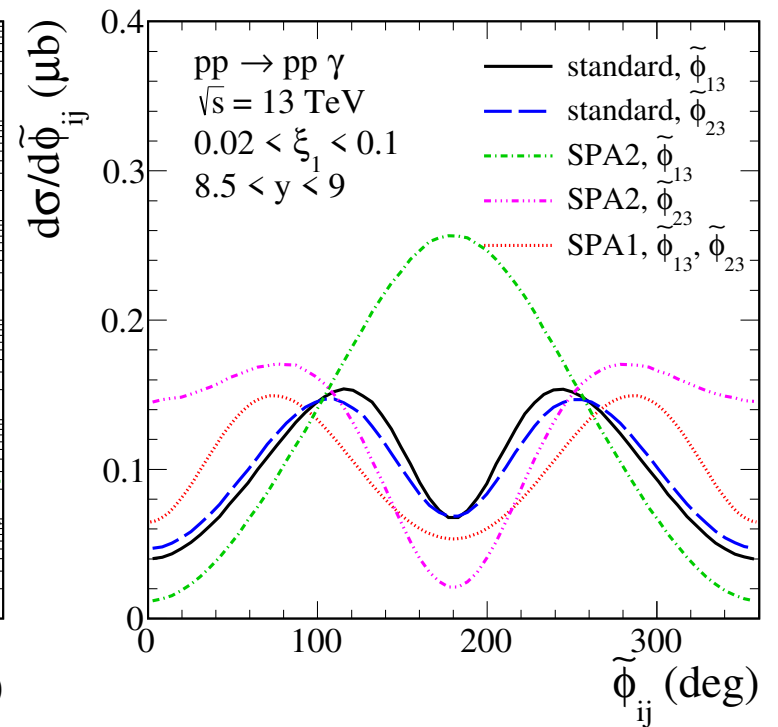
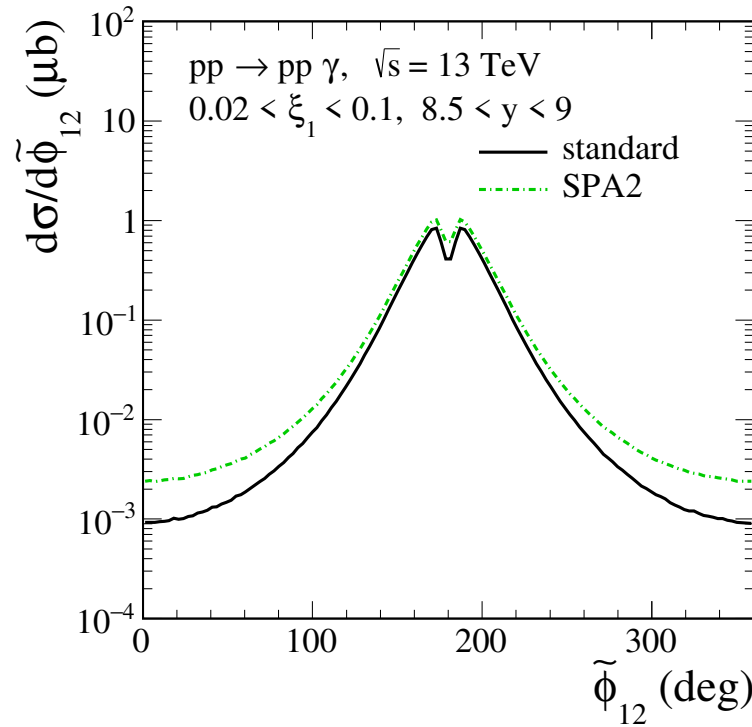
$pp \rightarrow pp\gamma$, $\sqrt{s} = 13$ TeV, $0.02 < \xi_1 < 0.1$
 $d^2\sigma/dk_\perp dy$ ($\mu\text{b}/\text{GeV}$)



$pp \rightarrow pp\gamma$, $\sqrt{s} = 13$ TeV, $0.02 < \xi_1 < 0.1$
 $d^2\sigma/d\omega dy$ ($\mu\text{b}/\text{GeV}$)



Results, $pp \rightarrow pp\gamma$



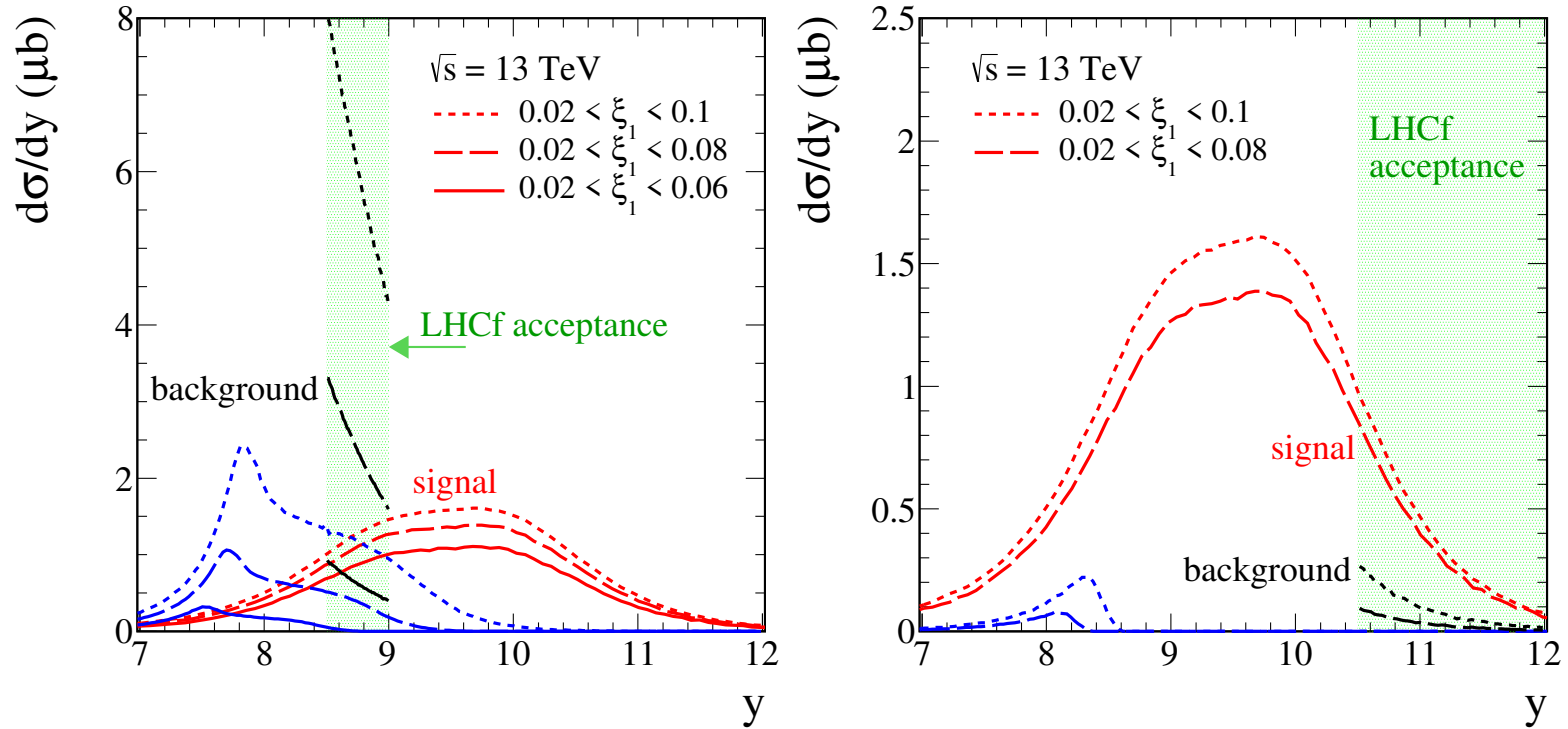
- The azimuthal angle correlations between outgoing particles

$$\tilde{\phi}_{ij} = \phi_i - \phi_j \mod(2\pi), \quad 0 \leq \tilde{\phi}_{ij} < 2\pi$$

are different for standard (exact) approach and for the SPA1 and SPA2 approaches.

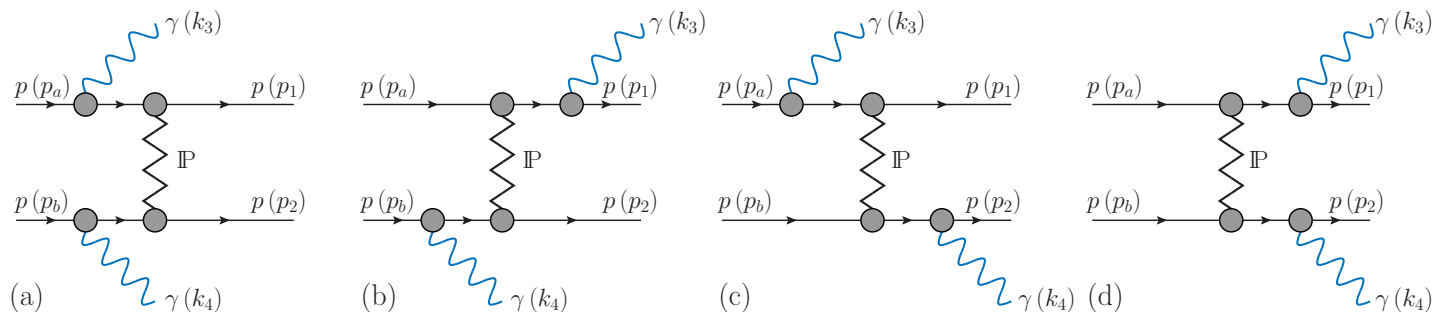
- For SPA1 the outgoing protons are back-to-back $\tilde{\phi}_{12} = \pi$ (not shown here).
- The SPA2 results for the azimuthal angles between proton and photon (right panel) deviate very significantly from our standard results.

Results, $pp \rightarrow pp\gamma$



- Signal and background contributions in two LHCf acceptance regions. For the background contribution we show the distributions of both photons from the decay of π^0 .
Background: $pp \rightarrow pp\pi^0$, DHD-type model based on [Lebiedowicz, Szczurek PRD87 \(2013\) 074037](#).
- One can increase the signal-to-background ratio to about 1 for the first LHCf acceptance region ($8.5 < y < 9$). For the second acceptance region ($y > 10.5$) the ratio > 3.5 .
- In order to isolate our signal reaction it would be very helpful if the transverse momenta of the outgoing protons and photon could be measured.

$pp \rightarrow pp\gamma\gamma$

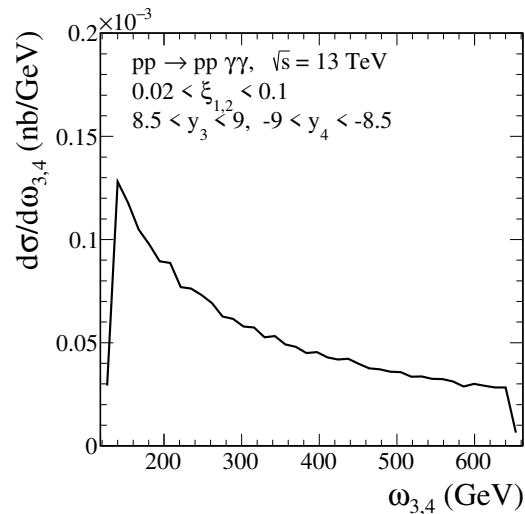
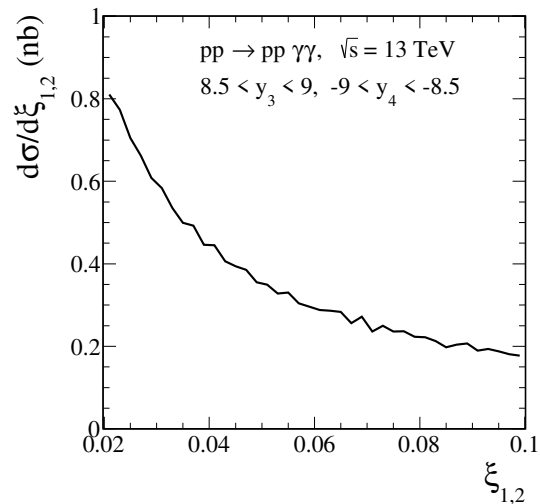


$$\begin{aligned} \mathcal{M}_{\mu\nu, \text{SPA1}} &= e^2 \mathcal{M}^{(\text{on shell}) pp}(s, t) \\ &\times \left[-\frac{p_{a\mu}}{(p_a \cdot k_3)} + \frac{p_{1\mu}}{(p_1 \cdot k_3)} \right] \\ &\times \left[-\frac{p_{b\nu}}{(p_b \cdot k_4)} + \frac{p_{2\nu}}{(p_2 \cdot k_4)} \right] \end{aligned}$$

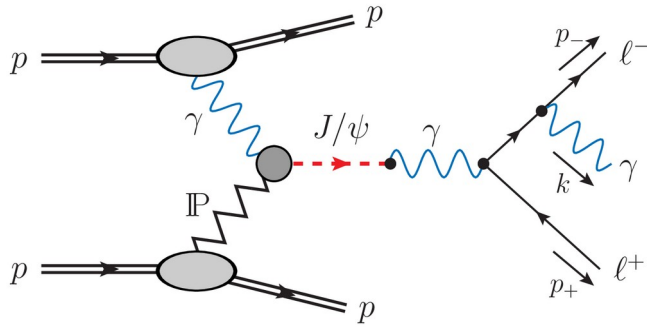
Fot cuts:

$8.5 < y_3 < 9, -9 < y_4 < -8.5$ (LHCf),
 $0.02 < \xi_{1,2} < 0.1$ (AFP)

$\sigma \simeq 0.03 \text{ nb}$ for $\sqrt{s} = 13 \text{ TeV}$



$$\xi_{1,2} = \frac{k_{\perp 3}}{\sqrt{s}} \exp(\pm y_3) + \frac{k_{\perp 4}}{\sqrt{s}} \exp(\pm y_4)$$



$$pp \rightarrow pp (J/\psi \rightarrow \mu^+ \mu^- \gamma)$$

The amplitude $\mathcal{M}_\mu^{(\gamma\mathbb{P})}$ is obtained as for $pp \rightarrow pp\phi$ but with $i\Gamma_\kappa^{(\phi KK)}(p_3, p_4)$ replaced by

$$\mathcal{M}^{(2 \rightarrow 5)} = (\epsilon^\mu(k))^* \mathcal{M}_\mu$$

$$\mathcal{M}_\mu = \mathcal{M}_\mu^{(\gamma\mathbb{P})} + \mathcal{M}_\mu^{(\mathbb{P}\gamma)}$$

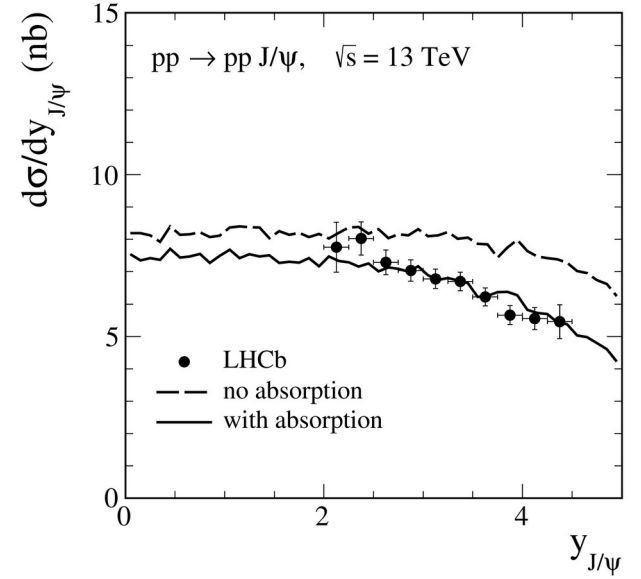
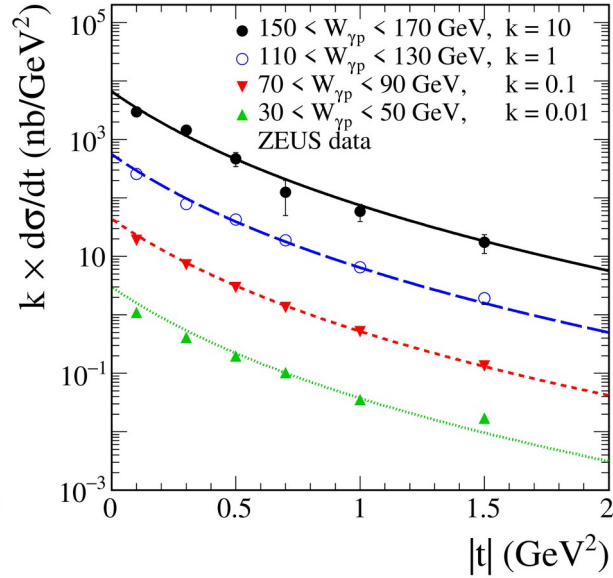
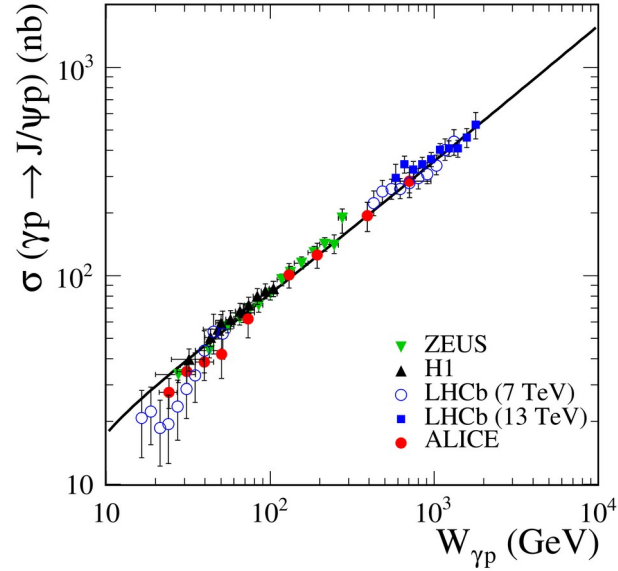
$$eg_{J/\psi\mu^+\mu^-} \bar{u}(p_-) \left(\frac{2p_- \cdot \mu + \gamma_\mu \not{k}}{2p_- \cdot k} \gamma_\kappa - \gamma_\kappa \frac{2p_+ \cdot \mu + \not{k} \gamma_\mu}{2p_+ \cdot k} \right) v(p_+),$$

$g_{J/\psi\mu^+\mu^-} = 8.197 \times 10^{-3}$ is estimated from the decay rate $J/\psi \rightarrow \mu^+ \mu^-$.

In the following we shall compare the full decay approach to the approach where we keep only the pole terms $\propto \omega^{-1}$ in the radiative amplitude.

The \mathcal{M}_μ amplitude is then expressed by $\mathcal{M}_\mu \propto \mathcal{M}^{(2 \rightarrow 4)} e \left(\frac{p_- \cdot \mu}{p_- \cdot k} - \frac{p_+ \cdot \mu}{p_+ \cdot k} \right)$.

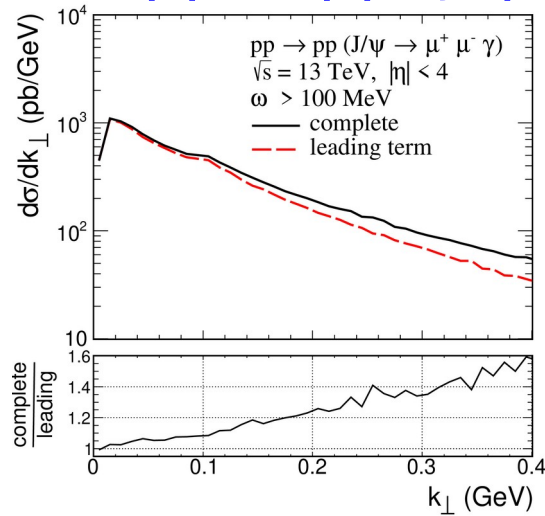
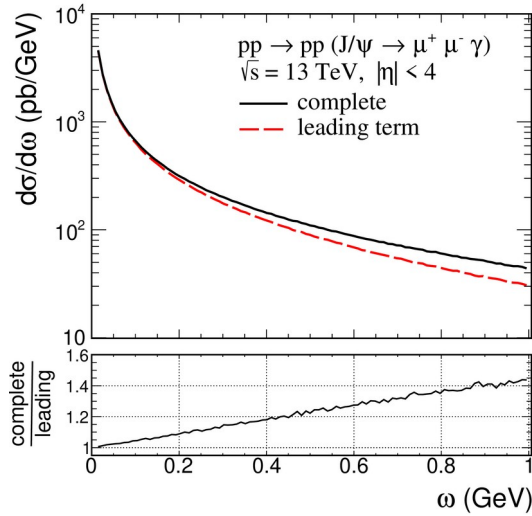
The $pp \rightarrow pp (J/\psi \rightarrow \mu^+ \mu^- \gamma)$ reaction is calculated within exact $2 \rightarrow 5$ kinematics using [GenEx event generator](#) [Kycia, Turnau, Chwastowski, Staszewski, Trzebiński, Commun. Comput. Phys. 25 (5) (2019) 1547]



The values of the intercept and slope parameters of the pomeron trajectory, the coupling constants, and the form-factor parameters were determined from a comparison of the model to the experimental data for the $\gamma p \rightarrow J/\psi p$ reaction.

The model supplemented by the absorptive corrections (pp rescattering) describes the LHCb data for $pp \rightarrow pp J/\psi$ [LHCb Collaboration, Aaij et al., JHEP 10 (2018) 167].

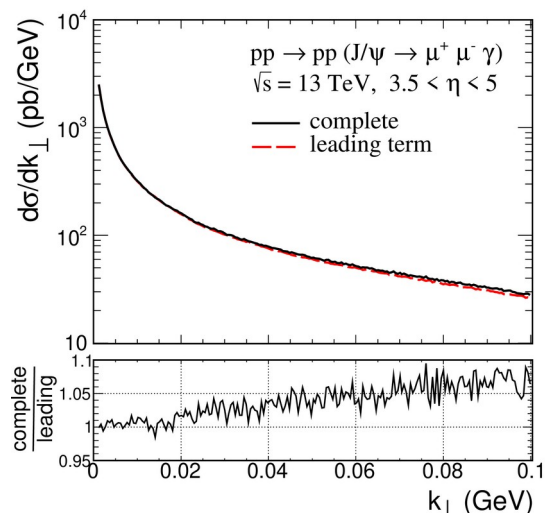
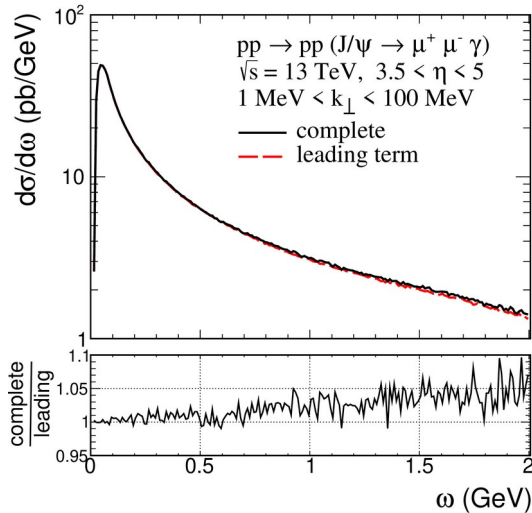
$pp \rightarrow pp (J/\psi \rightarrow \mu^+ \mu^- \gamma)$



Distributions in ω , the energy of the photon, and in k_\perp , the transverse momentum of the photon.

For soft-photon emission, the leading term in the decay dominates.

The other terms have no singularity for $k \rightarrow 0$.



See the report: R. Bailhache *et al.*, Anomalous soft photons: Status and perspectives, Phys. Rept. 1097 (2024) 1,

which summarizes the work of the EMMI RRTF on “Real and Virtual Photon Production at Ultra-Low Transverse Momentum and Low Mass at the LHC”

$pp \rightarrow pp (J/\psi \rightarrow \mu^+\mu^-\gamma)$

Table 1: The results have been calculated for $\sqrt{s} = 13$ TeV and for some acceptance cuts for ALICE 3. Both photons and muons cover the same pseudorapidity range. No absorption (pp rescattering) effects are included here.

$pp \rightarrow pp(J/\psi \rightarrow \mu^+\mu^-)$	σ (pb)	
no cuts	3458.2	
$ \eta < 1$	304.5	
$ \eta < 4$	2671.5	
$4 < \eta < 5$	68.8	
$pp \rightarrow pp(J/\psi \rightarrow \mu^+\mu^-\gamma)$	σ (pb), leading term	σ (pb), full decay
$\omega > 100$ MeV, $ \eta < 1$	8.8	12.3
$\omega > 100$ MeV, $ \eta < 4$	147.8	188.3
$\omega > 100$ MeV, $4 < \eta < 5$	5.9	6.6
$10 \text{ MeV} < \omega < 1 \text{ GeV}$, $ \eta < 4$	269.4	290.2
$k_\perp > 1$ MeV, $3.5 < \eta < 5$	18.3	19.8
$1 \text{ MeV} < k_\perp < 10 \text{ MeV}$, $3.5 < \eta < 5$	7.4	7.4
$10 \text{ MeV} < k_\perp < 100 \text{ MeV}$, $3.5 < \eta < 5$	7.0	7.2
$100 \text{ MeV} < k_\perp < 1 \text{ GeV}$, $3.5 < \eta < 5$	3.9	5.2
$k_\perp > 100$ MeV, $ \eta < 1$	8.1	11.6
$k_\perp > 100$ MeV, $ \eta < 4$	75.8	113.1

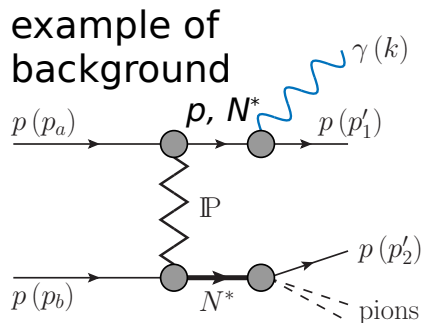
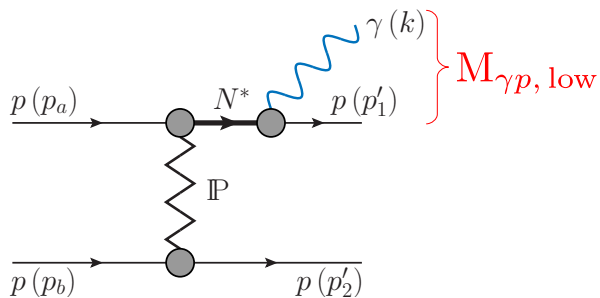
Note that the cut on k_\perp significantly reduces the cross section compared to that of the cut on ω , especially at forward photon rapidities

Summary

- We have studied **soft-photon bremsstrahlung** at forward photon rapidities and various CEP processes in proton-proton collisions at the LHC. At midrapidities, the photoproduction mechanism for $pp \rightarrow p\gamma$ gives a much larger cross section than bremsstrahlung. We have compared our standard (exact) bremsstrahlung results and the results using soft-photon approximations (SPAs).
- To calculate the amplitudes the framework of the **tensor-pomeron model** was used. It is effective model where some parameters have to be determined from experiment.
- **The single photon bremsstrahlung mechanism should be identifiable by the measurement of proton (AFP) and photon (LHCf) on one side and by checking the exclusivity condition** (no particles in the ATLAS detector) without explicit measurement of the opposite side proton. Whether this is sufficient requires further studies, since such a measurement will probably include one-side diffractive dissociation, which can be of the order of 30%. **We have estimated the coincidence cross section** (within SPA1) **for $pp \rightarrow p\gamma\gamma$** where photons are emitted in opposite sides of the ATLAS interaction point and can be measured by two different arms of LHCf. The cross section is rather small but should be measurable.
- For detailed comparison of our predictions with experiment (**ALICE 3, ATLAS-LHCf**), and in order to distinguish our exact bremsstrahlung and SPA results, measurement of outgoing protons would be welcome. **Next Generation Facilities at the LHC** will be able to measure photons in coincidence with protons in the forward detectors, as discussed in:
 - EMMI RRTF Workshop on “Real and Virtual Photon Production at Ultra-Low Transverse Momentum and Low Mass at the LHC”, report: R. Bailhache *et al.*, Anomalous soft photons: Status and perspectives, Phys. Rept. 1097 (2024) 1
 - EMMI RRTF Workshop on “Next Generation Facility for Forward Physics at the LHC”, 17-21 Feb 2025, Heidelberg (report in preparation)

Backup

Comments on diffractive excitations of the protons (N^* resonances)



- N^* candidates are (satisfy the Gribov-Morrison rule):
 $N(1440) J^P=1/2^+$, $N(1520) J^P=3/2^-$, $N(1680) J^P=5/2^+$

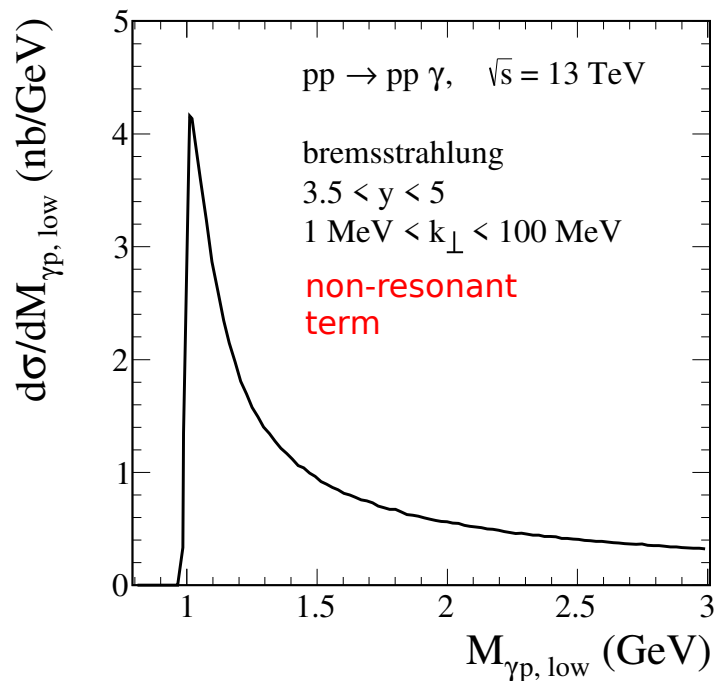
$$\text{BR}(N(1440) \rightarrow p\gamma) \sim 0.04 \%$$

$$\text{BR}(N(1520) \rightarrow p\gamma) \sim 0.3 - 0.5 \%$$

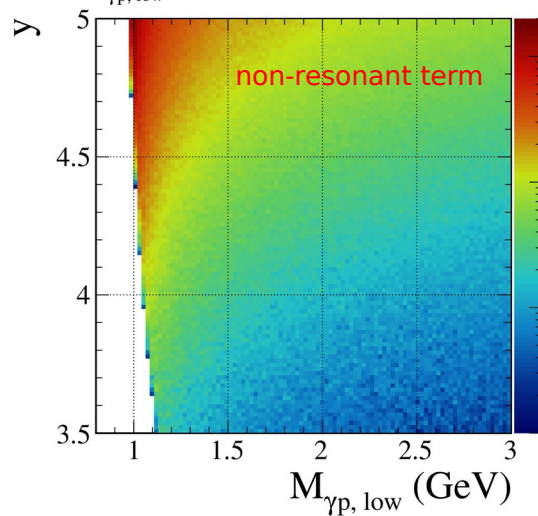
$$\text{BR}(N(1680) \rightarrow p\gamma) \sim 0.2 - 0.3 \%$$

\leftarrow a sizeable cross section
 $pp \rightarrow pN(1680)$ was estimated at CERN ISR @ 45 GeV

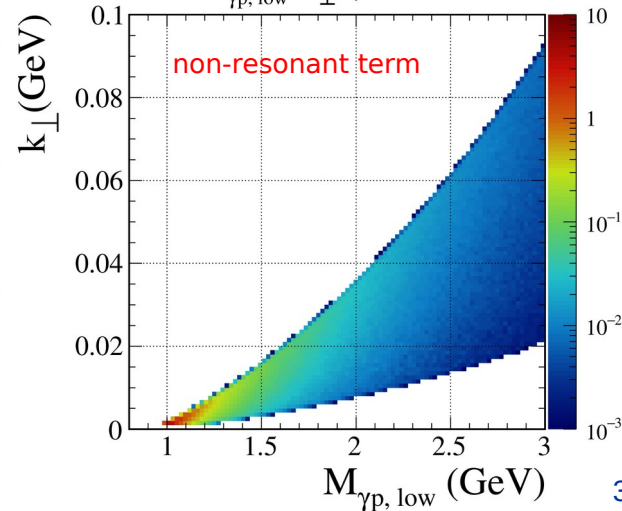
- If these processes contribute significantly to our reaction then we should see them in the $M_{\gamma p, \text{low}}$ distribution (possibly distorted by interference effects) as a resonance enhancement at $M_{\gamma p} = m_{N^*}$ over the non-resonant term



$pp \rightarrow pp \gamma$, $\sqrt{s} = 13 \text{ TeV}$, $1 \text{ MeV} < k_{\perp} < 100 \text{ MeV}$
 $d^2\sigma/dM_{\gamma p, \text{low}} dy$ ($\mu\text{b/GeV}$)



$pp \rightarrow pp \gamma$, $\sqrt{s} = 13 \text{ TeV}$, $3.5 < y < 5$
 $d^2\sigma/dM_{\gamma p, \text{low}} dk_{\perp}$ ($\mu\text{b/GeV}^2$)



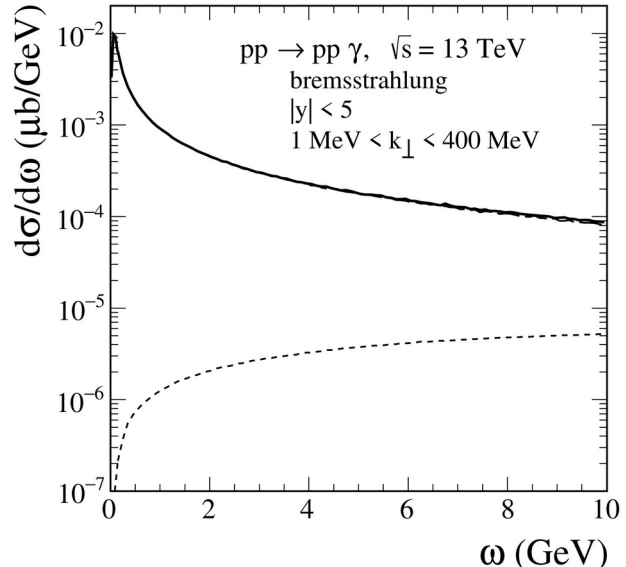
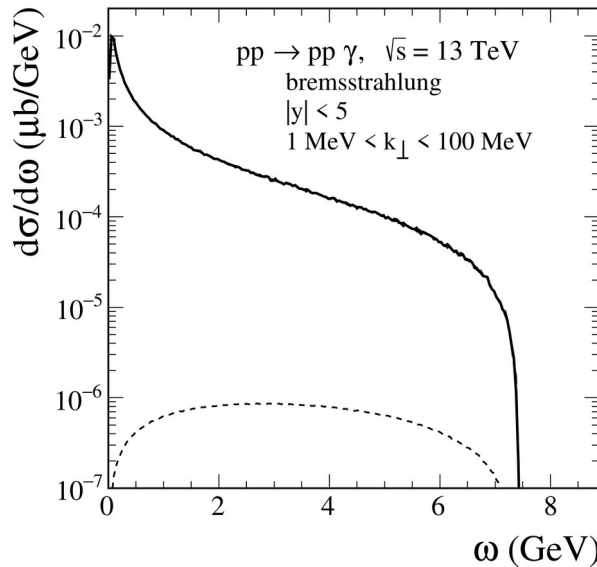
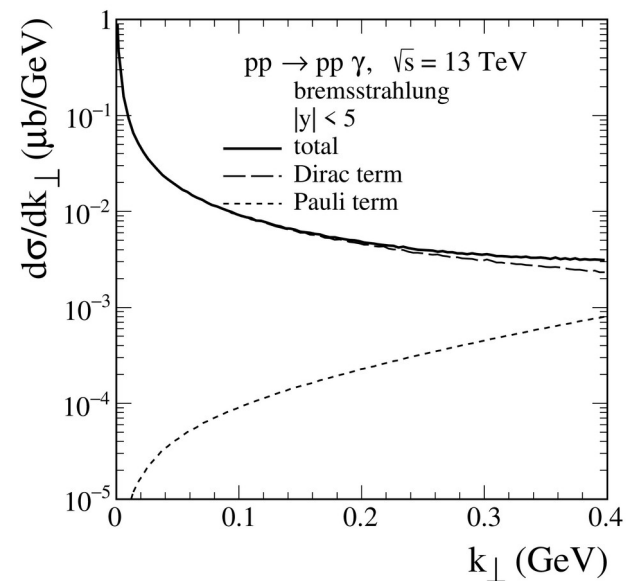
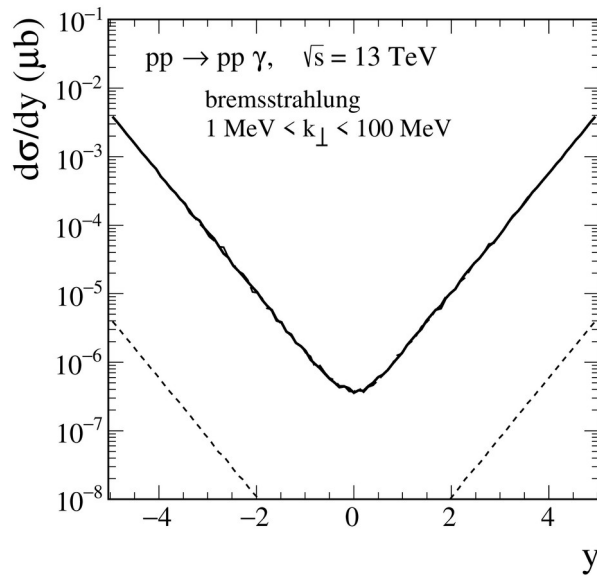
Bremsstrahlung

- In small k_{\perp} and ω regions the Dirac term from γpp vertex function dominates while for larger values the Pauli term (anomalous magnetic moment of the proton) plays an important role.

For the complete result all contributions to

$$\mathcal{M}_{\mu}^{(\text{standard})}$$

with Dirac and Pauli terms have to be added coherently.



Bremsstrahlung

- Results for
 $6 < y < 13$
 $0.02 < \xi_1 < 0.1$

